Biotechnology Advances 30 (2012) 108–130

Contents lists available at SciVerse ScienceDirect

Biotechnology Advances

journal homepage: www.elsevier.com/locate/biotechadv

Sic1 plays a role in timing and oscillatory behaviour of B-type cyclins

Matteo Barberis [a,*], Christian Linke [b,c,1], Miquel À. Adrover [d,1], Alberto González-Novo [d], Hans Lehrach [b], Sylvia Krobitsch [b], Francesc Posas [d], Edda Klipp [a]

[a] Institute for Biology, Theoretical Biophysics, Humboldt University Berlin, Invalidenstraβe 42, 10115 Berlin, Germany
[b] Max Planck Institute for Molecular Genetics, Ihnestraβe 73, 14195 Berlin, Germany
[c] Department of Biology, Chemistry and Pharmacy, Free University Berlin, Takustraβe 3, 14195 Berlin, Germany
[d] Cell Signaling Unit, Departament de Ciències Experimentals i de la Salut, Universitat Pompeu Fabra, Dr. Aiguader 88, 08003 Barcelona, Spain

ARTICLE INFO

Available online 18 September 2011

Keywords:
Cell cycle
Oscillations
Cyclin waves
B-type cyclins
Sic1
Budding yeast

ABSTRACT

Budding yeast cell cycle oscillates between states of low and high cyclin-dependent kinase activity, driven by association of Cdk1 with B-type (Clb) cyclins. Various Cdk1–Clb complexes are activated and inactivated in a fixed, temporally regulated sequence, inducing the behaviour known as “waves of cyclins”. The transition from low to high Clb activity is triggered by degradation of Sic1, the inhibitor of Cdk1–Clb complexes, at the entry to S phase. The G_1 phase is characterized by low Clb activity and high Sic1 levels. High Clb activity and Sic1 proteolysis are found from the beginning of the S phase until the end of mitosis. The mechanism regulating the appearance on schedule of Cdk1–Clb complexes is currently unknown. Here, we analyse oscillations of Clbs, focusing on the role of their inhibitor Sic1. We compare mathematical networks differing in interactions that Sic1 may establish with Cdk1–Clb complexes. Our analysis suggests that the wave-like cyclins pattern derives from the binding of Sic1 to all Clb pairs rather than from Clb degradation. These predictions are experimentally validated, showing that Sic1 indeed interacts and coexists in time with Clbs. Intriguingly, a *sic1Δ* strain looses cell cycle-regulated periodicity of Clbs, which is observed in the wild type, whether a *SIC1-0P* strain delays the formation of Clb waves. Our results highlight an additional role for Sic1 in regulating Cdk1–Clb complexes, coordinating their appearance.

1. Introduction

Budding yeast cell cycle is driven by periodic changes in the activity of Cdk1 kinase, regulated by different pools of cyclins that associate with Cdk1 in successive waves (Fig. 1A, reviewed in Futcher, 1996). B-type cyclins Clb1–6 are expressed at different times and appear sequentially in specific cell cycle phases, resulting in a significant divergence of function (Bloom and Cross, 2007; Cross et al., 1999). Clb5,6 rise at the beginning of S phase and function primarily in the control of DNA replication (Schwob and Nasmyth, 1993; Schwob et al., 1994; Spellman et al., 1998). Clb3,4 increase in mid-S phase at about the same time as spindle pole bodies separate and their specific function is still unclear (Fitch et al., 1992; Richardson et al., 1992). Clb1,2 rise as mitotic spindle assembly progresses and are involved in the control of mitotic exit (Deshaies, 1997; Fitch et al., 1992; Spellman et al., 1998). The regulation of active Cdk1–Clb complexes involves a combination of positive feed-forward loops – depending on the regulated transcription of *CLB* genes (Bloom and Cross, 2007; Fitch et al., 1992; Koch and Nasmyth, 1994) – and negative feedback loops – via down-regulation of Clb levels via ubiquitin/26S proteasome pathway (Amon et al., 1994; Hochstrasser, 1995; Irniger et al., 1995; King et al., 1996; Lew and Reed, 1995; Seufert et al., 1995; Tyers and Jorgensen, 2000).

The transcriptional regulation of Clbs is a fine-tuned mechanism (Fig. 1B, reviewed in Bloom and Cross, 2007). *CLB5,6* transcription is promoted by the Mbp1/Swi6 Binding Factor (MBF) (Schwob and Nasmyth, 1993), and interactions of Clb5,6 with Swi4/6 Binding Factor (SBF) and MBF have been reported (Pic-Taylor et al., 2004; Simon et al., 2001). *CLB1,2* transcription is controlled by the Fkh2 forkhead transcription factor during G_2/M phase (Kumar et al., 2000; Reynolds et al., 2003) and both Cdk1–Clb5 and Cdk1–Clb2 interact with, and phosphorylate, Fkh2 to control Clb1,2 accumulation (Hollenhorst et al., 2000; Pic-Taylor et al., 2004; Ubersax et al., 2003; Yeong et al., 2001) (Fig. 1B, arrows C and D, respectively). No information is available so far about the activation of *CLB3,4* transcription. The only study reported to date is a genome-wide location analysis to identify binding sites for transcription factors, which suggested that the Fkh1 forkhead transcription factor binds to Clb4 (Simon et al., 2001). Moreover, Fkh1 binds to the *CLB4* promoter (CCDB database, Alfieri et al., 2007).

The degradation of Clbs by proteolysis is a highly specific mechanism (Fig. 1C), with the consequence that Cdk1 is inactivated. Clb6 is the only B-type cyclin to be directed to degradation by the ubiquitin

* Corresponding author. Tel.: +49 30 2093 8383; fax: +49 30 2093 8813.
E-mail addresses: matteo.barberis@biologie.hu-berlin.de (M. Barberis), edda.klipp@rz.hu-berlin.de (E. Klipp).

[1] These two authors contributed equally to the present study.

0734-9750/$ – see front matter © 2011 Elsevier Inc. All rights reserved.
doi:10.1016/j.biotechadv.2011.09.004

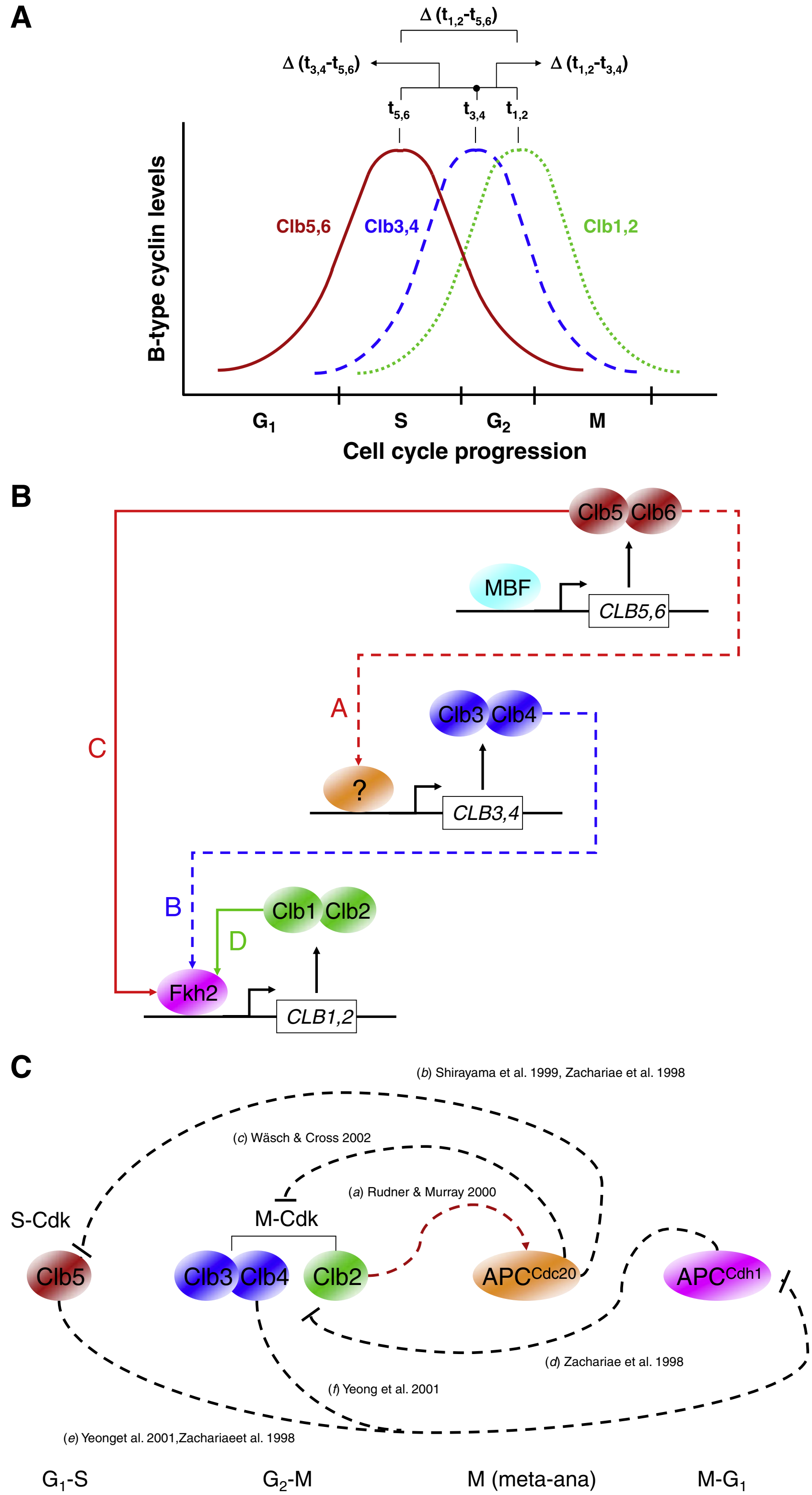

Fig. 1. Mechanisms of regulation of B-type cyclins. (A) Qualitative description of waves of Clbs during the cell cycle. Time distances between the peaks of Clbs, mentioned in the text, are also visualized: $t_{3,4}-t_{5,6}$ represents the time delay between Clb5,6 and Clb3,4, $t_{1,2}-t_{5,6}$ the time delay between Clb5,6 and Clb1,2 and $t_{1,2}-t_{3,4}$ the time delay between Clb3,4 and Clb1,2. (B) Transcriptional regulation of Clbs. Cdk1–Clb5,6 promote *CLB3,4* transcription (A), Cdk1–Clb3,4 promote *CLB1,2* transcription (B) together with Cdk1–Clb5,6 (C), and Cdk1–Clb1,2 promote *CLB1,2* transcription by stimulating its own production (D). For simplicity, Cdk1 subunit has been omitted. See text for details. (C) Clb-regulated degradation. Phosphorylation of Cdc20 by Cdk1–Clb2 activates APC^{Cdc20} (*a*). APC^{Cdc20} targets Clb5 for degradation (*b*) and degrades also mitotic cyclins (*c*). APC^{Cdh1} degrades Clb2 further during mitotic exit and in the following G_1 phase (*d*). Phosphorylation of Cdh1 by Cdk1–Clb5 (*e*) and by Cdk1-Clb3,4 (*f*) inactivates APC^{Cdh1}, thereby permitting the subsequent accumulation of Clb2. Bibliographic references are also indicated.

ligase complex, SCF (Skp1/Cullin/F-box), before the degradation of Clb5 (Jackson et al., 2006). The other B-type cyclins are ubiquitinated by the Anaphase Promoting Complex (APC) (Peters, 2006). This mechanism of degradation occurs through the mutual regulation of two forms of APC, APC^{Cdc20} and APC^{Cdh1}, which are differentially regulated by Cdk1–Clb-mediated phosphorylation (Shirayama et al., 1999; Wasch and Cross, 2002).

The sequential activation and degradation of Clbs gives directionality to cell cycle events. In addition, Sic1, a specific stoichiometric inhibitor of Cdk1–Clb complexes and structural and functional homolog to 27^{Kip1} in mammalian cells (Barberis et al., 2005a), contributes to their regulation (Schwob et al., 1994). Sic1 is synthesized at the end of mitosis and largely degraded at the onset of S phase in an SCF-dependent manner (Schwob et al., 1994; Verma et al., 1997b). Cdk1–Cln1,2 and Cdk1–Clbs phosphorylate Sic1 (Nash et al., 2001; Nasmyth, 1996; Verma et al., 1997b), which results in Sic1 being recognized by the protein degradation machinery. In early G_1 phase, Cdk1 activity is abolished by low levels of *CLB* expression, by high levels of Sic1 and by the APC^{Cdh1}-mediated ubiquitination of Clbs. Because Clns are neither inhibited by Sic1 nor targeted by APC^{Cdh1}, Cdk1–Cln1,2-associated activity increases and phosphorylates Cdh1, thereby reducing APC activity. This event is accompanied by increased *CLB5,6* expression, resulting in Cdk1–Clb5,6 accumulation. The Clb5,6-associated kinase activity is initially inhibited by Sic1, producing a pool of inactive Cdk1–Clb5,6 that becomes active as soon as Sic1 starts to be targeted for degradation by Cdk1–Cln1,2 (Nash et al., 2001; Verma et al., 1997b). Destruction of Sic1 relieves Cdk1–Clbs inhibition and cells enter into S phase. In late G_1 phase, Cdk1–Clb5,6 contribute together with Cdk1–Cln1,2 to Cdh1 phosphorylation and, thus, to APC inactivation. Together with Sic1 degradation, this allows a gradual increase of active Clbs towards mitosis. Subsequent waves of Cdk1–Clb activity initiate entry into mitosis, and its completion occurs when mitotic Cdk1–Clb activates APC^{Cdc20}. Cdk1–Clb inactivation in late mitosis activates APC^{Cdh1} and prevents Sic1destruction, which begins to accumulate (Cross, 2003).

The involvement of Sic1 in cell cycle regulation is well recognized. However, there is a relevant controversy in the field regarding the specific phases where Sic1 functions. Despite data showing that Sic1 is largely degraded at the G_1/S transition to permit DNA synthesis (Schwob et al., 1994; Thornton and Toczyski, 2003; Verma et al., 1997b), *SIC1* transcription levels are observed throughout the entire cell cycle (Aerne et al., 1998; Knapp et al., 1996). Moreover, recent data show that yeast cells expressing a non-degradable form of Sic1 show a retard, but not an impairment, in the onset of DNA replication due to the delayed activation of the Cdk1–Clb activity, indicating that Sic1 does not have to be completely degraded to drive cell cycle progression (Cross et al., 2007). Nonetheless, time course experiments performed in G_1 cells synchronized by α-factor show that levels of Sic1 are detectable throughout the cell cycle (Archambault et al., 2003; Coccetti et al., 2004).

In this work, we show through a combination of mathematical modelling and experimentation that Sic1 is indeed continuously detected during the entire cell cycle, with the only exception of a temporal window in which all Clbs are present at the maximal level, and could play a role in coordinating the timing of Clbs waves.

2. Materials and methods

2.1. Description of temporal dynamics by ODEs

The dynamics are described by ordinary differential equations. We explicitly consider a single compartment, where dynamics of the concentration for every compound is determined by biochemical reactions. In Appendix A is listed the full set of equations used in this study. The parameters reported in Table A.1 are not derived from experimental data, but are suitable for simulating the experiments described. Importantly, all parameters used for the simulations have the same value within all networks.

2.2. Local sensitivity analysis

To test the impact of parameters on the dynamics, local sensitivity analysis is performed. Classical sensitivity analysis defines the sensitivity S as the change of a model output quantity O caused by the change of a parameter value p, i.e. $S=(\Delta O/O)/(\Delta p/p)$. Since we study the impact of parameter changes on concentration time courses, we performed sensitivity analysis by calculating the time-dependent response coefficients $R=(\partial c_i(t)/c_i(t))/(\partial p/p)$ (Ingalls and Sauro, 2003). These coefficients indicate the direction and amount of change of the time course for the concentration $c_i(t)$ upon an infinitesimal change of the parameter (or initial concentration) p. They allow tracing the effect of a parameter change on a concentration during the whole simulation period. The analysis focused on Cdk1**–**Clb complexes. Calculation of time-dependent response coefficients serve to test the influence of parameters on the timing and strength of response, confirming the consistency of the network structures.

2.3. Global sensitivity analysis

To analyse whether parameter values influence a specific property of the network, global sensitivity analysis is performed with a Monte Carlo approach. Random parameter sampling is employed to estimate the sensitivities of the network property "time delay between Clbs" with respect to parameters, without knowing their precise values. We randomly select 10,000 parameter sets and simulate in each case different variants of the network. In the analysis, all parameters of the network may vary between 0.1-fold and 10-fold of their initial values.

2.4. Programs and software

The networks are simulated with the software Mathematica® Version 5.1, Wolfram Research.

2.5. Yeast strains and growth media

For yeast-two-hybrid analyses the strain L40ccua (*MAT*a *his3*-200 *trp1*-901 *leu2*-3,112 *LYS2*::(lexAop)4-*HIS3 ura3*::(lexAop)8-lacZ *ADE2*::(lexAop)8-*URA3 gal80* canR cyh2R) was used. For GST pull-down assays we manipulated the *SIC1* gene in the BY4741 strain background (*MAT*a *his3Δ1 leu2Δ0 met15Δ0 ura3Δ0*) by using one-step PCR-mediated gene targeting procedure (Longtine et al., 1998). To amplify the integration cassette we used the pYM18 vector containing the 9-Myc tag (accession number P30304, PCR-Toolbox, Euroscarf) as template and primers as listed in Table A.2. To perform time course experiments two isogenic BY4741 derivative strains were used, YAN48 (*CLB3-TAP:HIS3*, *SIC1-TAP:KanMX::Nat*, *CLB2-18MycKl:KanMx::URA3*, *CLB5-6HA:KanMx*), generated by tagging one of each of Clb pairs along with Sic1, and YAN68 (*CLB3-TAP:HIS3*, *sic1::HPH*, *CLB2-18MycKl:KanMx::URA3*, *CLB5-6HA:KanMx*), obtained by swapping the *SIC1-TAP:KanMX::Nat* genomic construction on YAN48 by a cassette containing the Hygromycin B kinase gene (*HPH*). YAN48 cells were transformed either with the vector pMAD26 (*pRS415-GAL1::HA-SIC1-0P*), that over-expresses a metastable allele of *SIC1* lacking all nine phosphorylation sites for Cdk-cyclin-associated activity, or with the vector pAGN50 (*pRS415-GAL1::HA-SIC1*), that over-expresses a wild type *SIC1*. In this last case, YAN48 background was modified by swapping the *CLB2-18MycKl:KanMx::URA3* genomic construction by a cassette containing the leucine gene (*LEU2*). Yeast cells were grown at 30 °C in YPD on appropriate synthetic complete (SC) drop-out media. Low-phosphate medium was prepared by dissolving 5 g $(NH_4)_2SO_4$, 0.1 g NaCl, 20 g glucose and 1.6 g of the requested amino acids in 1 liter of water (Sherman, 2002).

2.6. Plasmids

For the generation of yeast-two-hybrid plasmids DNA fragments were amplified with specific primer pairs (see Table A.2) by PCR using genomic DNA isolated from BY4741 as template and Phusion High-Fidelity DNA Polymerase Kit, NEB. Resultant DNA fragments were purified and subcloned into the cloning vector pJET1.2/blunt (CloneJET PCR Cloning Kit, Fermentas). Clones were sequenced and subsequently subcloned into the bait (pBTM117, *TRP1* marker) and prey (pACT4, *LEU* marker) plasmids by recombinant cloning via *Sal*I / *Not*I restriction sites. For the generation of glutathione S-transferase (GST) fusion proteins for pull-down experiments coding sequences of *CLB1-6* genes were cloned into the vector pGEX2T via *Sal*I / *NotI* restriction sites.

2.7. Centrifugal elutriation

YAN48 and YAN68 cells were grown in rich medium (YPD) to OD = 4.5 (OD = 3 for YAN86) and synchronized by centrifugal elutriation using a JE-5.0™ rotor mounted on a Avanti J-25™ centrifuge (Beckman Coulter). Cells were loaded into rotor directly from saturated culture, YPD was used as elutriation buffer and the system was kept at 30 °C during the elutriation process. After stabilization and recovery of middle-sized G_1 cells (or small newborn cells in the case of YAN68) from elutriation cells were concentrated to OD = 0.5 by vacuum-driven filtering using a Durapore Membrane Filter™ with 0.45 μm of pore diameter (Millipore). Cells were then transferred to fresh YPD at 30 °C, grown during 30 min (or 60 min for YAN68) for recovery before the first sample was taken (time = 0). For *SIC1-0P* over-expression YAN48 cells transformed with the vector pMAD26 were grown on SD medium plus 2% raffinose to OD = 2.5. Newborn cells were recovered from similar elutriation in SD 2% raffinose and equally filtered to be concentrated to OD = 0.5 either in fresh SD 2% raffinose or SD 1% raffinose plus 1% galactose without any recovery time (time = 0).

2.8. Western blot, cytometry analysis and budding index

TCA protein extracts were resolved on SDS-PAGE buffer, blotted to an Immobilon Membrane™ (Millipore). Total Clb2, Clb3, Clb5 and Sic1 levels were detected sequentially by incubating with mouse α-HA, α-Myc, and α-PAP without stripping the membrane, in the way that detection of proteins was done at the same time by chemoluminescence. Total Cdk1 was detected aside as loading control using the anti-PSTAIRE antibody. For flow cytometry analysis cells were fixed in 70% ethanol and treated overnight with RNAse A at 37 °C in 50 mM sodium citrate. DNA was stained with propidium iodide and analysed in a FACScan Flow Cytometer™ (Becton Dickinson). A total of 10,000 cells were analysed and the fraction of G_1 cells quantified for each time point using WinMDI 2.9. Budding index (% of budded cells) was scored by microscopy (n = 300).

For the comparison between *SIC1-0P* and *SIC1* over-expressions YAN48 cells transformed with the vectors pMAD26 and pAGN50, respectively, were grown overnight on raffinose medium lacking uracil. Cultures were split, washed twice and half of each culture was resuspended on either glucose or galactose containing media. Cells were incubated at 30 °C for 5 h and fixed for microscopic inspection. Fixed cells were stained with DAPI and observed under an epifluorescence microscope. 1 ml of each culture was also collected and added to 300 μl of TCA. TCA extracts were resolved in a 10% SDS-PAGE followed by western blot anti-HA. Hog1 was detected as a loading control.

2.9. Yeast-two-hybrid analysis

L40ccua cells were transformed with respective bait and prey plasmids, as described (Ralser et al., 2005a, 2005b). Transformants were selected on synthetic complete medium lacking amino acids tryptophan and leucine (SDII). Single colonies were then isolated and spotted onto synthetic complete medium lacking tryptophan, leucine, histidine and uracil (SDIV) as well as onto nylon membranes (Magna Charge Nylon Transfer membrane, Micron Separation Inc.). 2.5 mM 3-amino-1,2,4-triazole was added to SDIV media to measure the relative strength of interactions. The growth of transformants was monitored after plates had been incubated for 3–5 days at 30 °C. The activity of ß-galactosidase was determined as described (Ralser et al., 2005a, 2005b).

2.10. GST pull-down assay

E. coli cells (XL1blue or DH5α) carrying the different pGEX2T-Clb constructs were inoculated in LB media until OD_{600} = 0.5–07 and, subsequently, expression of proteins was induced by adding isopropylbeta-D-thiogalactopyranoside (IPTG, Fermentas) at a final concentration of 1 mM. After 3 h cells were harvested by centrifugation (7 min, 3000 rcf, 4 °C), pellets were dissolved in GST-binding buffer (TrisHCl 20 mM pH 7.9, NaCl 125 mM, $MgCl_2$ 5 mM, DTT 0.5 mM) and 10 mg/ml of Lysozym (Sigma Aldrich) was added. After sonication, 10% Glycerol and 0.1% NP-40 were added and cell lysates centrifuged (25 min, 20,000 rcf, 4 °C). The supernatants containing expressed GST-Clb proteins were incubated with Glutathione Sepharose 4B beads (GE Healthcare) for 8 h at 4 °C. Then, beads were washed with GST-binding buffer and incubated with 1 ml yeast protein lysate (5 μg/μl total protein) expressing Myc-tagged Sic1 overnight at 4 °C. The lysate was prepared from 200 ml YPD culture with OD_{600} = 1.2 by harvesting cells by centrifugation (4 min, 3000 rcf, 4 °C). Then, cells were washed with phosphate-buffered saline (PBS; NaCl 137 mM, KCl 2.7 mM, Na_2HPO_4 10 mM, KH_2PO_4 2 mM pH 7.4), frozen in liquid nitrogen, and lysed with glass beads (Sigma Aldrich, acid washed) by vigorous shaking. After centrifugation (1 min, 10,000 rcf, 4 °C) cell lysate was used for pull-down experiments. Finally, samples from pull-down experiments were washed twice with ice-cold GST-binding buffer, bound proteins were eluted with SDS sample buffer and loaded on 10% SDS-gel. After transfer onto a nitrocellulose Protran membrane (PerkinElmer), the membrane was treated with rabbit α-myc antibody (1:l, Sigma Aldrich) followed by incubation with the corresponding peroxidase (POD)-coupled secondary antibody (1:5000, α-rabbit IgG POD conjugate, Sigma Aldrich) and proteins were visualized with Western Lighting luminol reagent (PerkinElmer) by exposing to a High performance chemiluminescence film (GE Healthcare).

3. Results

3.1. Mathematical network of Cdk1–Clb regulation

The features of cell cycle control can be reproduced with mathematical models (Barberis et al., 2007; Chen et al., 2000, 2004). Through modelling of the G_1/S transition in budding yeast we provided an explanation for a dual role of Sic1 in triggering cell cycle events: as a negative regulator of Cdk1–Clb complexes, and promoter of Cdk1–Clb5,6 entry into the nucleus to start DNA replication (Barberis and Klipp, 2007; Barberis et al., 2007).

To investigate whether Sic1 plays a potential role in the regulation of the oscillatory behaviour of Clbs, we systematically compared networks that differ in interactions between Sic1 and Cdk1–Clbs. For this purpose, we made assumptions for the activation of Cdk1–Clbs, one after the other, based on literature data. First, after *CLB5,6* transcription by MBF, we considered that Cdk1-Clb5,6 activate *CLB3,4* transcription via an unknown transcription factor, possibly Fkh1 (Fig. 1B, arrow A, k_A). A direct involvement of Cdk1-Clb5,6 in the activation of *CLB3,4* promoters is suggested from the following data: (i) *CLB3,4* can partially compensate for the lack of *CLB1,2* genes (Fitch et al., 1992) and functionally compensate for defects in the Mcm1-forkhead regulatory system (Kumar et al., 2000), and (ii) Cdk1-Clb5 regulates *CLB2* transcription leading to the Mcm1-forkhead complex activation. Second, we considered that Cdk1-Clb3,4 activate *CLB1,2* transcription via the Fkh2 transcription factor (Fig. 1B, arrow B, k_B). Fkh2 phosphorylation is not abolished in the absence of Clb5, suggesting that other Clb-kinases are capable of this role. This is supported by the following findings: (i) in the absence of Clb3, Clb4 and Clb5, *CLB2* promoter is not fully active and Clb2 is highly unstable (Yeong et al., 2001), and (ii) Fkh2 phosphorylation is reduced but not abolished by loss of Clb5 (Pic-Taylor et al., 2004). Thus, Cdk1-Clb3,4 could play a role in Fkh2 phosphorylation. Moreover, according to the transcriptional regulation of Clbs reported in literature (see Introduction), Clb1,2 accumulation is promoted by phosphorylating Fkh2 *via* both Cdk1–Clb5 (Fig. 1B, arrow C, k_C) and Cdk1–Clb2 (Fig. 1B, arrow D, k_D).

The first signalling network investigated is shown in Fig. 2, implemented by a set of ordinary differential equations (ODEs) presenting the dynamic behaviour of Cdk1-Clbs in time (see Appendix A). The full set of parameters is reported in Table A.1. After basal production of Cdk1–Clb5,6 (k_1) (synthesis regarded as constant, unregulated), Sic1 binds to it forming the Cdk1–Clb5,6-Sic1 ternary complex (k_2), which is also dissociated (k_3). When Sic1 is degraded first by Cdk1–Cln1,2 (k_5) and secondarily by all Cdk1–Clbs, C1 (Cdk1–Clb5,6), C2 (Cdk1–Clb3,4) and C3 (Cdk1–Clb1,2) (k_5), Cdk1–Clb5,6 promote Cdk1–Clb3,4 activation (k_A), in addition to its basal production (k_7). Clb5,6 in the Cdk1–Clb5,6-Sic1 ternary complex are also degraded (k_4). For simplicity, we did not include the explicit role of Cdk1–Cln1,2 on Sic1 degradation (Nash et al., 2001; Verma et al., 1997b), but we incorporated it as a basal activity in the reaction rate k_5. In the following, Cdk1–Clb3,4 promote Cdk1-Clb1,2 activation (k_B) together with Cdk1–Clb5,6 (k_C), in addition to its basal production (k_9). Moreover, Cdk1–Clb1,2 promote their activation by a positive feedback loop (k_D). The basal degradation of Clb5,6, Clb3,4, Clb1,2 and Sic1 (k_6, k_8, k_{10} and k_{26}, respectively) is also considered. The network explicitly incorporates regulation of Cdk1-Clbs production (k_1, k_7, k_9), lumping together the processes from gene transcription to complex formation into a single step. For simplicity, in the first networks presented (Figs. 2 and B.9) we have not included the regulated Clb degradation, which instead will be considered in the last network (see Fig. 6).

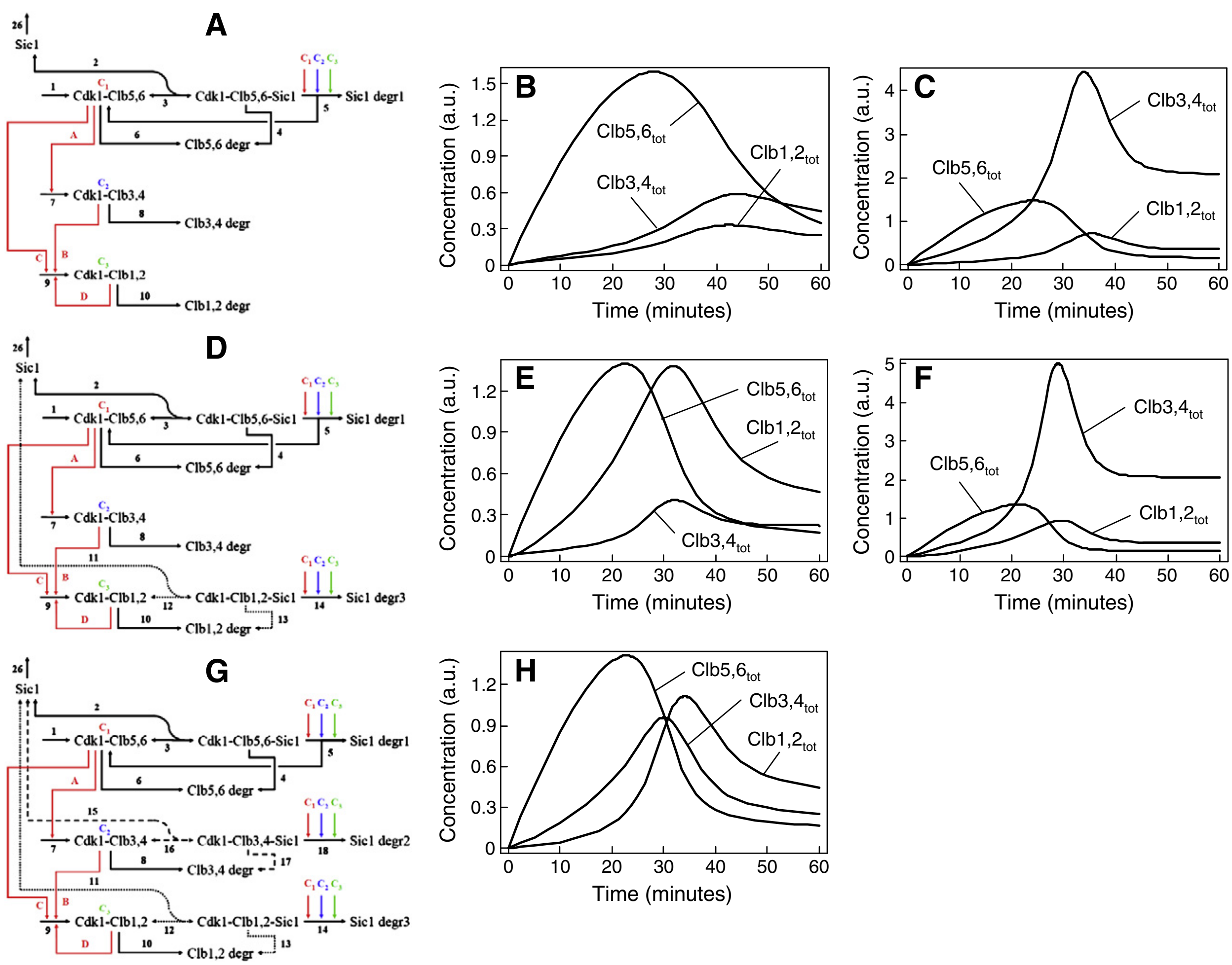

Fig. 2. Signalling network describing Cdk1–Clb regulation and computational time courses of Clb total levels. (A) Network describing the binding of Sic1 to Cdk1–Clb5,6 (solid lines). The sequential transcriptional activation of Cdk1–Clb complexes is shown in red (k_A, k_B, k_C and k_D). C1, C2 and C3 indicate Cdk1–Clb5,6, Cdk1–Clb3,4 and Cdk1–Clb1,2, respectively. See text for details. Simulations are carried out with standard values (B) or varying k_A, k_B and k_C (C), as reported in the text. (D) Network describing the binding of Sic1 to both Cdk1–Clb5,6 and Cdk1–Clb1,2 (dotted lines). Simulations are carried out with standard values (E) or varying k_A, k_B and k_C (F). (G) Network describing the binding of Sic1 to Cdk1–Clb5,6, Cdk1–Clb1,2 and Cdk1–Clb3,4 (dashed lines). Simulations are carried out with standard values (H). In all simulations, the initial concentration of Sic1 is set to 5, whereas all other initial concentrations are set to 0.

3.2. Computational analysis of temporal dynamics

We analysed three versions of the first signalling network, which encompasses different regulatory interactions that Sic1 can establish with Cdk1–Clbs (Fig. 2). In the first version, Sic1 binds only to Cdk1–Clb5,6 (solid lines) and, when Sic1 is degraded, Cdk1–Clb5,6 is active (Fig. 2A). In Fig. 2B computed time courses of total levels of Clb5,6, Clb3,4 and Clb1,2, i.e. the sum of all complexes in which each Clb is present, are shown. The simulations revealed no temporal coordination between the times of Clbs appearance. Varying specific parameters, e.g. increasing the effect of Cdk1–Clb5,6 on Cdk1–Clb3,4 activation (k_A from 100 to 1000), and decreasing the influence of both Cdk1–Clb5,6 and Cdk1–Clb3,4 on Cdk1–Clb1,2 activation (k_C from 100 to 10 and k_B from 1000 to 100, respectively), permitted to increase the maximum level for all complexes (Fig. 2C). However, no clear temporal distinction between Clb3,4 and Clb1,2 was observed, i.e. there was no delay in the appearance of their maximum levels (Fig. 2C). To confirm this observation, we tested the impact of k_A, k_B and k_C on the time delay between maximum levels of Clb3,4 and Clb1,2 (see Appendix B, Fig. B.1). A range of the values is considered for k_A (from 50 to 500), k_B (from 500 to 5000) and k_C (from 50 to 500). The maximum delay between Clb3,4 and Clb1,2 is reached when both k_A and k_B or k_A and k_C are small, whereas the minimum delay (or maximum overlap) is given when both k_A and k_B or k_A and k_C are high. Different values of k_B may give a pronounced delay. The results highlight that the difference in timing between Clb3,4 and Clb1,2 onset is due to the Clb5,6 effect (k_A and k_C) on the transcription of mitotic cyclins, rather than to Clb3,4-mediated activation of Clb1,2 (k_B). Moreover, we verified the dependence of the same parameters on time delays between all other combinations of Clbs (see Appendix B, Figs. B.2–B.7). For each analysis, panels A, B and C represent simulations for the networks depicted in Figs. 2, B.9 and 6, respectively: $t_{3,4} - t_{5,6}$, time delay between Clb5,6 and Clb3,4 (Figs. B.2 and B.5); $t_{1,2} - t_{3,4}$, time delay between Clb3,4 and Clb1,2 (Figs. B.3 and B.6); $t_{1,2} - t_{5,6}$, time delay between Clb5,6 and Clb1,2 (Figs. B.4 and B.7).

In the second version of the network, we introduced more details and considered the binding of Sic1 to both Cdk1–Clb5,6 and Cdk1–Clb1,2 (Fig. 2D, solid and dotted lines, respectively). This is in agreement with different studies that reported the interaction between Sic1 and Clb2 (Archambault et al., 2004; Bailly and Reed, 1999; Honey et al., 2001). In addition to the network presented in Fig. 2A, Sic1 binds to Cdk1–Clb1,2 forming the Cdk1–Clb1,2-Sic1 complex (k_{11}), which is also dissociated (k_{12}). Both Clb1,2 and Sic1 in the ternary complex are degraded (k_{13} and k_{14}, respectively). As shown in Fig. 2E, no temporal coordination between maximum levels of Clb5,6, Clb3,4 and Clb1,2 was observed. Increasing k_A and decreasing both k_B and k_C did not result in a differentiation between maximum levels of Clb3,4 and Clb1,2 (Fig. 2F). However, we observed a similar increase of the maximum level of Clb1,2 as compared to the previous simulation (see Fig. 2C and F), even if Clb1,2 and Clb3,4 still appeared at the same time.

Finally, we addressed the interaction between Sic1 and Cdk1–Clb3,4. The scheme in which Sic1 binds to, and regulates the equilibrium of, all Cdk1-Clbs is shown in Fig. 2G (solid, dotted, and dashed lines). This assumption is in agreement with high throughput genome-wide screenings for complexes, where Sic1 was associated to Clb3 (Archambault et al., 2004; Breitkreutz et al., 2010; Collins et al., 2007; Gavin et al., 2006; Krogan et al., 2006) and Clb4 (Breitkreutz et al., 2010; Collins et al., 2007), but these interactions have never been validated independently. In addition to the network presented in Fig. 2D, Sic1 binds to Cdk1–Clb3,4 forming the Cdk1-Clb3,4-Sic1 complex (k_{15}), which is also dissociated (k_{16}). Both Clb3,4 and Sic1 in the ternary complex are degraded (k_{17} and k_{18}, respectively).This specific sequence of molecular interactions reproduced the oscillation-like behaviour of the phase-specific Clbs (Fig. 2H) (Fitch et al., 1992; Koch and Nasmyth, 1994). The different time delays of Clb appearance are listed in Appendix B, Table A.3. To test the impact of the choice of parameter values on the dynamic behaviour, a local sensitivity analysis on the formation of Cdk1–Clb5,6, Cdk1–Clb3,4 and Cdk1–Clb1,2 has been performed (see Appendix B, Fig. B.8). Calculation of time-dependent response coefficients served to test the influence of rate constants and initial concentrations on timing and strength of the response, finding agreement between sensitivities and network structure. Importantly, all common parameters used for the simulation were the same for the three versions of the network shown in Fig. 2. Small and medium variations of those parameters did not change our conclusion: Sic1 can be the potential key regulator through a feed-forward mechanism generating the waves of Clb levels, and the staggered timing of their appearance.

Also an increase in the granularity of the model by introducing intermediate unregulated steps to generate a delay between the appearance times of Clbs provides a similar result. In fact, taking into account the steps that contribute to Clbs formation, i.e. production of Clb3,4 and Clb1,2 from gene to protein and formation of Cdk1–Clb complexes, the waves of cyclin behaviour was obtained only when Sic1 was bound to all Cdk1–Clbs (see Appendix B, Fig. B.9 and figure legend for model details). The different time delays of Clb appearance are listed in Appendix B, Table A.3. Local sensitivity analysis has been also performed, observing agreement between the sensitivities and the network structure (see Appendix B, Fig. B.10).

3.3. Global sensitivity analysis of the network

To address whether the delay between the appearance of Clb5,6, Clb3,4 and Clb1,2 was due to the specific parameter choice, we performed a global sensitivity analysis with a Monte Carlo type approach by varying all parameters of the network presented in Fig. 2G between 0.1-fold and 10-fold of their initial values (see Materials and methods). We compared versions of the network shown in Fig. 2, where Sic1 either binds to Cdk1–Clb5,6 only (version 1, Fig. 2A), to both Cdk1–Clb5,6 and Cdk1–Clb1,2 (version 2, Fig. 2D) or to all three kinase complexes (version 3, Fig. 2G). The pairwise comparison of time delays of Clbs appearance between different versions – in which versions 1 and 2 are analysed in comparison to version 3 – is shown in Fig. 3. The analysis of the time delay between maximum levels of Clb5,6 and Clb3,4 showed that change of parameter values affects this distance almost to the same extent in both versions 1 and 3 (Fig. 3A). A similar result was observed in the comparison of versions 2 and 3 (Fig. 3B). The analysis of the time delay between maximum levels of Clb5,6 and Clb1,2 (Fig. 3C and D) showed the same tendency as observed for the distance between maximum levels of Clb5,6 and Clb3,4. If Sic1 did not bind to both Cdk1-Clb3,4 and Cdk1–Clb1,2 (version 1) or to Cdk1–Clb3,4 (version 2), time delays of the separation between Clb3,4 and Clb1,2 tended to be smaller (Fig. 3E and F). Remarkably, we observed a clear effect on the temporal distance between Clb3,4 and Clb1,2, being the correlation indexes gravely diminished with respect to parameter values of the network. Any change of the parameters affected the delay of Clb appearance more clearly only when Sic1 is bound to all Cdk1–Clb complexes (version 3).

From these analyses we conclude that regulation of time delays between Clbs is essentially triggered by interaction of Sic1 with all Cdk1–Clb complexes. Importantly, the interaction of Sic1 to Clb3,4 leads to a temporal separation between Clb3,4 and Clb1,2.

3.4. Sic1 interacts with all B-type cyclins

To further investigate the role of Sic1 in regulating the temporal appearance of Clbs, we investigated experimentally whether Sic1 can interact with all of them. Associations of Sic1 with all B-type cyclins have been detected in high throughput genome-wide

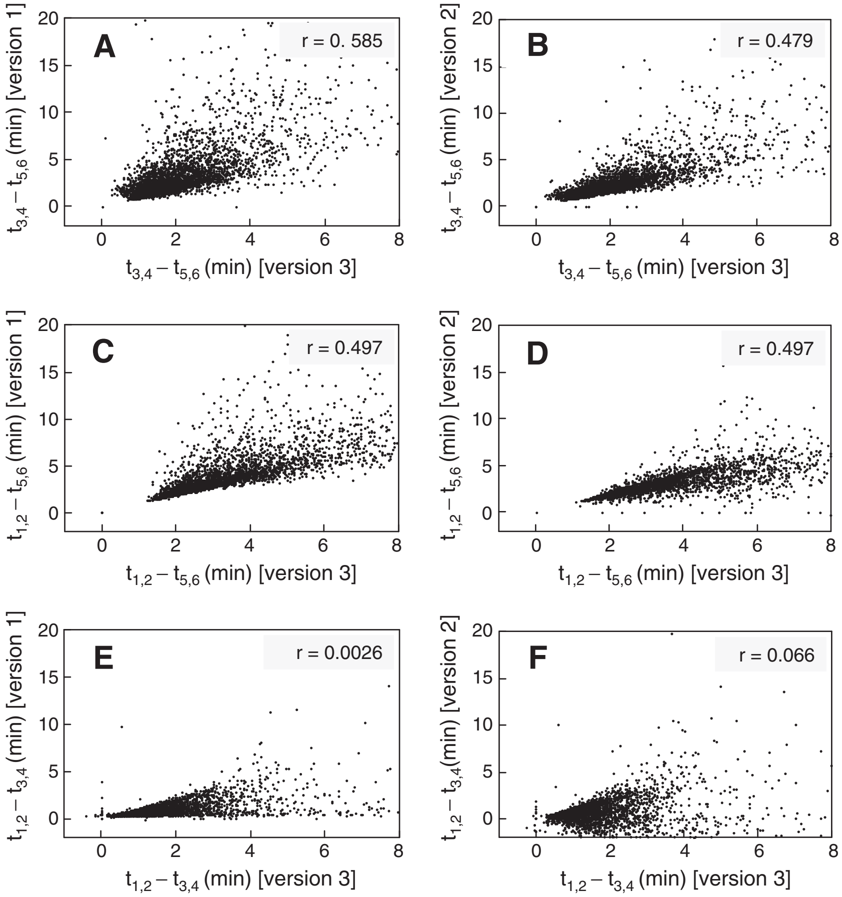

Fig. 3. Impact of the network parameter values on the delay between Clbs appearance. The graphs report the time delay observed between maximum levels of Clbs for binary combinations of the three network variants reported in Fig. 2. (A, B) Time delay between Clb5,6 and Clb3,4 ($t_{3,4}-t_{5,6}$). (C, D) Time delay between Clb5,6 and Clb1,2 ($t_{1,2}-t_{5,6}$). (E, F) Time delay between Clb3,4 and Clb1,2 ($t_{1,2}-t_{3,4}$). Each parameter of the network may vary from his selected value to the same value multiplied for a random real value comprised between 0.1 and 10.

screenings for complexes (Archambault et al., 2004; Bailly and Reed, 1999; Breitkreutz et al., 2010; Collins et al., 2007; Cross and Jacobson, 2000; Gavin et al., 2006; Honey et al., 2001; Krogan et al., 2006; Verma et al., 1997a) and the interactions with Clb2 and Clb5 are well established, but to our knowledge interactions with other Clbs have not been independently validated yet.

For this purpose, directed yeast-two-hybrid analysis was performed (Fig. 4). We generated bait (pBTM117) and prey (pACT4) constructs for Sic1 and Clbs, and transformed different combinations in yeast. We observed that yeast cells expressing fusion proteins LexA-Sic1 (pBTM-Sic1) and AD-Clb1–6 (pACT-Clb1–6) were able to grow on selective SDIV media, indicating activity of the reporter genes. No growth of yeast expressing control proteins LexA (pBTM) and AD (pACT), or LexA (pBTM) and AD-Clb1–6 (pACT-Clb1–6) was observed on SDIV, excluding activation of reporter genes per se (Fig. 4A). To investigate the relative strength of interactions, 3-amino-1,2,4-triazole (3′AT) was added to the media. Only yeast cells expressing fusion proteins LexA-Sic1 (pBTM-Sic1) and AD-Clb4 (pACT-Clb4), or at a lesser extent AD-Clb1 (pACT-Clb1), were able to grow on selective 3′AT medium (Fig. 4A), suggesting that these interactions might be stronger compared to other Sic1–Clb interactions. To further demonstrate the specificity of the interaction between Sic1 and Clbs, yeast-two-hybrid analysis with the unrelated Pbp1 protein (Mangus et al., 1998) was performed. As expected, no growth for fusion proteins LexA-Pbp1 (pBTM-Pbp1) and AD-Clb1-6 (pACT-Clb1-6) was observed on SDIV media (data not shown). Therefore, we conclude that interactions between Sic1 and all Clbs are specific.

In a next step, we investigated whether the observed interaction between Sic1 and Clbs can be also validated by GST pull-down analysis (Fig. 4B). To this end, we generated glutathione S-transferase (GST) fusion proteins for *CLB1–6* genes. Proteins were immobilized on Glutathione Sepharose beads and incubated with yeast lysate containing recombinant Myc-tagged Sic1. We observed that Sic1-Myc (~46 kDa) co-precipitated with all GST-tagged Clbs (lanes 4 and 5), but not with Sepharose beads alone (lane 2) or with GST-coupled resins (lane 3).

Our experimental results, together with the indication that Sic1 is substrate for the Clb3-associated kinase activity (data not shown) as it has been reported for Clb5 and Clb2 (Feldman et al., 1997; Skowyra et al., 1997; Ubersax et al., 2003), support the hypothesis that Sic1 might interact with all Cdk1–Clb complexes.

3.5. Sic1 coexists in time with all B-type cyclins and could coordinate their timing during cell cycle progression

To demonstrate that Sic1 does not coexist exclusively with Clb5,6 at the G_1/S transition and with Clb1,2 at the transition into anaphase (Schwob et al., 1994; Toyn et al., 1997) but also with Clb3,4 during cell cycle progression, we performed a time course experiment with G_1-elutriated cells.

We tagged one cyclin for each Clb pair (Clb2, Clb3 and Clb5) and Sic1 in a single yeast strain, synchronized the cells by elutriation and followed in time the waves of Clb levels together with Sic1 by Western blot (Fig. 5A). As previously described (Schwob et al.,

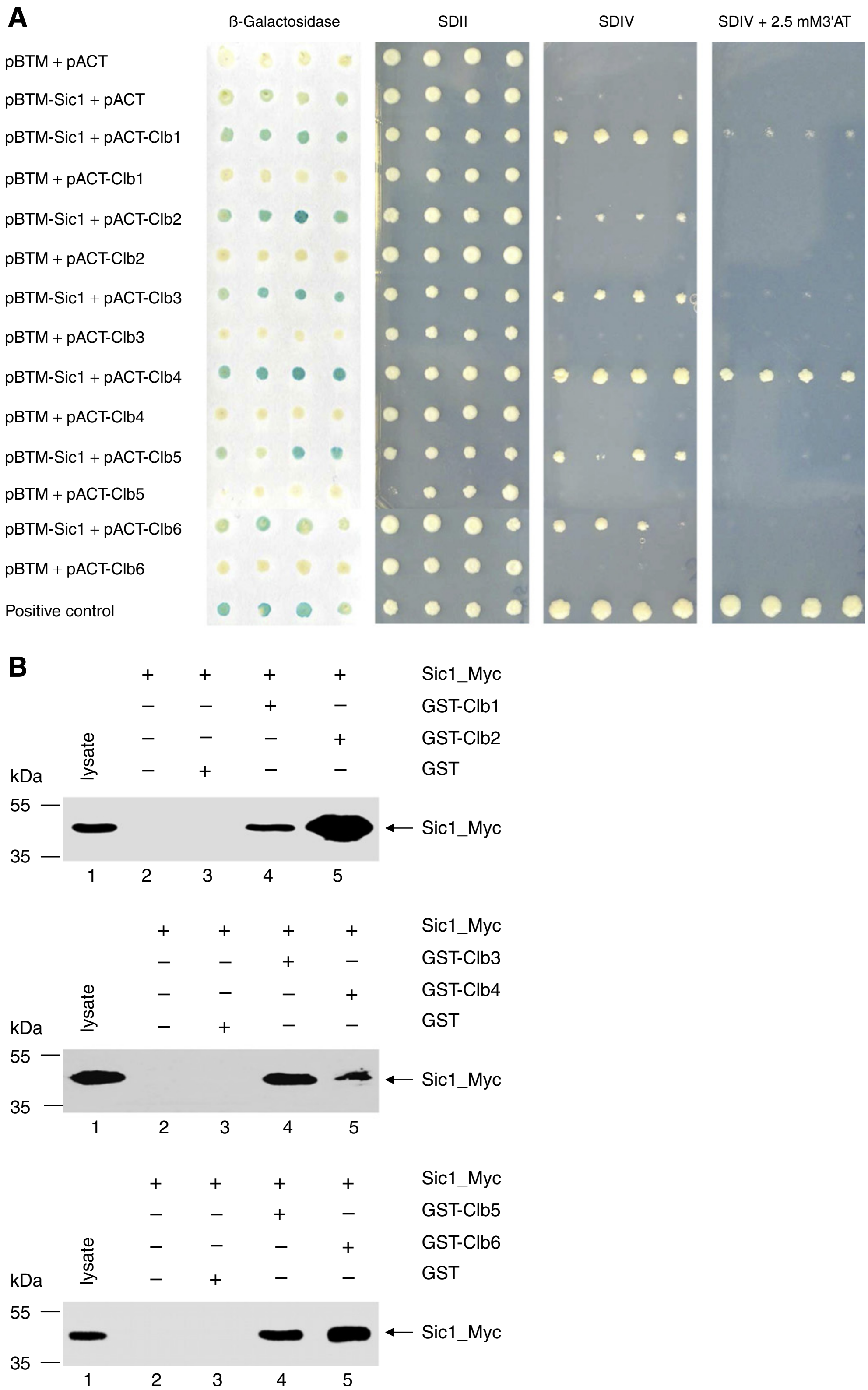

Fig. 4. Sic1 interacts with B-type cyclins. (A) Yeast cells expressing various fusion proteins (see text for details) were spotted onto selective media lacking the respective amino acids (SDII, SDIV) or on membrane for detection of β-galactosidase activity. 2.5 mM 3-amino-1,2,4-triazole (3′AT) was used to measure the relative strength of interactions. The interaction between the C-terminal domain of human ATXN2, ATXN2-FD, and the C-terminal domain of human PABP, PABC, was used as positive control. (B) Bacterial expressed proteins GST and GST-Clbs were immobilized on Glutathine Sepharose beads and incubated with lysate from yeast cells expressing Myc-tagged Sic1 from its endogenous promoter. Concentrated Sic1-Myc lysate served as a loading control (lane 1). Sepharose beads (lane 2) and GST-coupled resins (lane 3) were used as negative controls. Precipitation of Sic1-Myc bound on immobilized GST-Clb1,3,5 (lane 4) and GST-Clb2,4,6 (lane 5) was detected with rabbit α-Myc antibody (lanes 4 and 5).

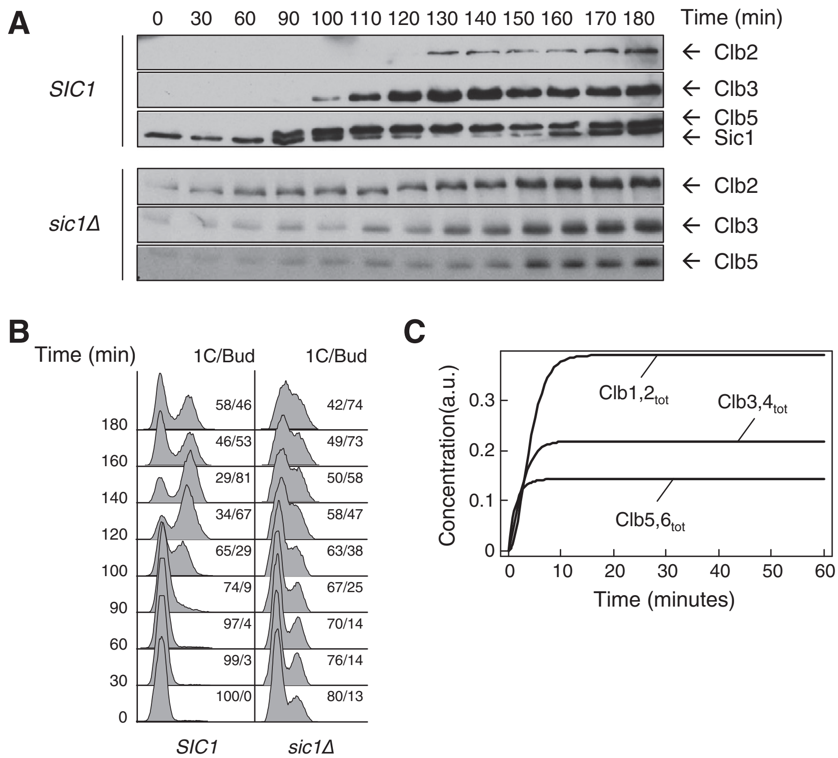

Fig. 5. Sic1 coexists with all B-type cyclins and potentially coordinates their correct timing along cell cycle. (A) Time course of Clb2, Clb3 and Clb5 in wild type (YAN48) and *sic1Δ* (YAN68) strains. Yeast cells were synchronized by centrifugal elutriation in YPD at 30 °C, released into fresh YPD at 30 °C, and sampled for Western blot analysis at the indicated times. The result is representative of four independent experiments. (B) Cell synchrony. The same time points reported in (A) were sampled to measure both DNA content by Flow Cytometry and budding by microscopy. (C) Simulation of the *sic1Δ* mutant. The simulation is carried out with standard values and with an initial concentration of Sic1 set to 0.

1994), Sic1 started to be degraded upon entry into S phase (between 100 and 120 min). Moreover, Clb5, Clb3 and Clb2 rise at 90, 100 and 130 min, respectively, showing the characteristic periodicity of Clb levels during cell cycle progression. We did not observe complete degradation of all Clb proteins, most probably due to loss of synchrony. However, drop in Clb2 levels corresponds to Sic1 increase and to the transition from meta- to anaphase (visible at 140–150 min), as confirmed by measuring the DNA content of samples taken during the elutriation, where cells proceed though citokinesis immediately afterwards (Fig. 5B). Sic1 and Clb3 were labelled with the same tag and detectable also at low levels. During both decline and rising of Sic1, Clb3 was present in relative high amounts (110 and 160 min), indicating that Sic1 coexists with Clb3 at different time points. Moreover, Sic1 was not completely degraded and its levels detectable until 140–150 min, length of one complete cell cycle, with the exception of the temporal window (130–140 min) where Sic1 reached its minimal levels and all Clbs peaked (Fig. 5A). This is in agreement with the general idea that all Cdk1-Clb complexes can contribute to maintain Sic1 at low levels until anaphase (Nasmyth, 1996). This aspect has been also implemented into the mathematical model, where Sic1 is degraded from each Cdk1–Clb–Sic1 ternary complex (see Fig. 2G).

Interestingly, a *sic1Δ* strain seems to lose the timing of Clbs appearance, although cells proceeded into the replicative state (Fig. 5A and B). Despite the lack of perfect synchrony of the strain, relative levels of Clb5, Clb3 and Clb2 appeared to be similar in all time points and progressively increased as compared to the wild type (Fig. 5A). In particular, Clb2 levels, which raised at 130 min in the wild type, accumulate already at time 0 in the *sic1Δ* strain, with cells arrested for the majority in G_1 phase (Fig. 5A and B). Simulation of the *sic1Δ* mutant qualitative agrees with this finding, showing that Clb waves are abolished and their levels reach different plateau, as observed experimentally (Fig. 5C). This result suggests that our predictions are valid, highlighting the fact that the model could reflect a mechanism existing in living cells to coordinate Clbs appearance.

3.6. Clb oscillations: Clb-stimulated degradation or Sic1-mediated regulation?

In the network of Cdk1–Clb regulation presented in Fig. 2, degradation of Clbs was simplified by setting fixed rate constants (reactions 5, 7 and 9). However, two APC complexes, APC^{Cdc20} and APC^{Cdh1}, are involved in the down-regulation of Clb levels (see Introduction). Fig. 6 shows largely the same network, taking additionally into account Clb degradation via APC according to Fig. 1C. For simplicity, APC complexes and their interactions with Clbs were not explicitly included. Instead, the role of specific Cdk1–Clb complexes in Clbs down-regulation, through activation or inactivation of APC, was included as indicated by arrows E, F, G and H. As for the other equations of the network, we described the APC-regulated degradation of Clbs using mass action kinetics. Specifically, we introduced: (i) Clb5,6 degradation stimulated by Cdk1–Clb3,4 and Cdk1–Clb1,2 (Fig. 6, arrows E and F – k_E and k_F – respectively), and (ii) Clb3,4 and Clb1,2 degradations stimulated by Cdk1–Clb1,2 (Fig. 6A, arrows G and H – k_G and k_H – respectively).

The computed time courses of total levels of Clb5,6, Clb3,4 and Clb1,2 resembled those obtained previously, showing no staggering between times of Clbs appearance. This was observed when Sic1 binds to Cdk1–Clb5,6 only (Fig. 6B), or to both Cdk1–Clb5,6 and Cdk1–Clb1,2 (Fig. 6E). Similarly, by modulating values of parameters k_A, k_B and k_C as previously described (Fig. 2), no differentiation between maximum levels of Clb3,4 and Clb1,2 was observed (Fig. 6C and F). Only the binding of Sic1 to all Cdk1–Clb complexes generated the time delay between Clbs (Fig. 6H). The different time delays of Clb appearance are listed in Appendix B, Table A.3. A local sensitivity

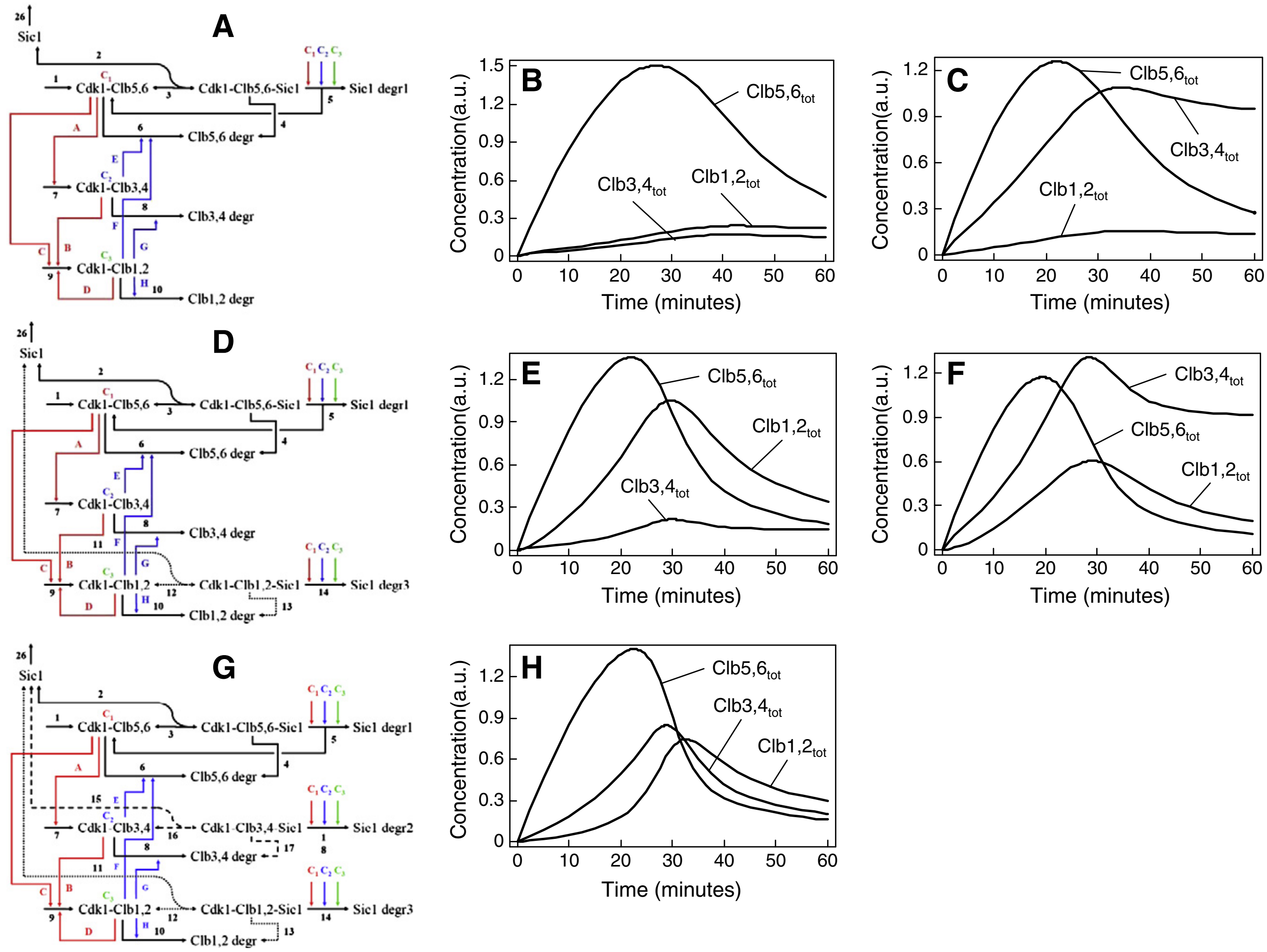

Fig. 6. Signallig network describing the Clb-regulated degradation and computational time courses of Clb total levels. (A) Network describing the binding of Sic1 to Cdk1–Clb5,6 (solid lines), based on the network shown in Fig. 2A. The Clb-regulated degradation by Cdk1–Clb complexes is shown in blue: Clb5,6 degradation is stimulated by both Cdk1–Clb3,4 (k_E) and Cdk1–Clb1,2 (k_F), Cdk1–Clb1,2 stimulates both Clb3,4 (k_G) and Clb1,2 (k_H) degradations. Simulations are carried out with standard values (B) or varying k_A, k_B and k_C (C), as reported in the simulations shown in Fig. 2. (D) Network describing the binding of Sic1 to both Cdk1–Clb5,6 and Cdk1–Clb1,2 (dotted lines). Simulations are carried out with standard values (E) or varying k_A, k_B and k_C (F). (G) Network describing the binding of Sic1 to Cdk1–Clb5,6, Cdk1–Clb1,2 and Cdk1–Clb3,4 (dashed lines). Simulations are carried out with standard values (H). In all simulations, the initial concentration of Sic1 is set to 5, whereas all other initial concentrations are set to 0.

analysis of the levels of Cdk1–Clb complexes with respect to parameter variations was also performed to check the agreement between sensitivities and network structure (see Appendix B, Fig. B.11).

These results suggest that waves of cyclins derive from a qualitative structural property of the network, i.e. binding of Sic1 to all three Clb pairs, rather than a quantitative property, such as Clbs degradation. In agreement with this finding, it has been reported that regulated Clbs proteolysis is not inherently essential because oscillations in Sic1 levels can substitute for APC as regulator of the Cdk1–Clb activity (Thornton and Toczyski, 2003). Moreover, a recent paper investigating the contribution of cyclin proteolysis to the irreversibility of mitotic exit showed that a feedback loop involving Sic1 is required to maintain low Cdk1–Clb2 activity and to prevent cyclin re-synthesis (Lopez-Aviles et al., 2009). This demonstrates that the unidirectionality of mitotic exit is not the consequence of Clb2 proteolysis and that cyclin degradation is not an absolute requirement for a viable cell cycle.

3.7. Effect of Sic1 degradation on Cdk1–Clb dynamics

Considering that oscillations in Sic1 levels trigger the feedforward loop necessary for the periodic changes in the Cdk1–Clb activity (Thornton and Toczyski, 2003), we investigated the role of Sic1 in the regulation of Cdk1–Clb complexes. We focused on the change in level of Sic1 phosphorylation and, thus, degradation. Multisite phosphorylation of Sic1 is a key process for entering into S phase at a correct timing, and mathematical description for this mechanism has been investigated (Borg et al., 2007; Deshaies and Ferrell, 2001; Gunawardena, 2005; Harper, 2002; Klein et al., 2003; Nash et al., 2001). Sic1 is promptly degraded at the G_1/S transition after initial phophorylation by Cdk1–Cln1,2 (Nash et al., 2001; Verma et al., 1997b) to release the activity of Cdk1–Clb5,6 required to start DNA replication (Schwob et al., 1994), and we also included this event in the mathematical model of the G_1/S transition (Barberis et al., 2007). Moreover, all Cdk1–Clb complexes could phosphorylate Sic1, therefore promoting its proteolysis, to maintain low levels until anaphase (Nasmyth, 1996), and we considered this potential mechanism in the networks presented in Figs. 2, B.9 and 6. Recent data suggested that a unphosphorylatable (non-degradable) form of Sic1 (*SIC-0P*) transiently blocks Cdk1–Clb activation, but that ultimately the total level of these complexes could increase above Sic1 level to drive cell cycle progression (Cross et al., 2007). Failure of Sic1 phosphorylation and proteolysis imposes a lengthened G_1 phase, variable delays in the budded part of the cell cycle and an extreme sensitivity to Clb dosage, rather than a lethal cell cycle block (Cross et al., 2007). This potentially indicates that stable Sic1 retards the onset of DNA replication due to a delayed activation of Cdk1–Clb activities.

To address this issue, we performed a time course experiment over-expressing the non- degradable form of Sic1 (*SIC1-0P*) under the *GAL* promoter in the same Clb-tagged strain used in Fig. 5. After cell synchronization by elutriation, we followed waves of Clb2, Clb3 and Clb5 levels in time by Western blot after release on raffinose or raffinose plus galactose media (Fig. 7A). In raffinose-growing cells, Clbs show their characteristic periodicity starting to accumulate progressively at 170 min (Clb5), 200 min (Clb3) and 210 min (Clb2). In this condition, DNA synthesis occurs at around 200 min, as shown by measuring the content of DNA of samples taken during the elutriation (Fig. 7B). Interestingly, the over-expression of *SIC1-0P* in this strain delays both timing of Clbs appearance and DNA replication onset (Fig. 7A and B), indicating that cell cycle delay observed by Cross and colleagues could be due to the retard in which different Clbs are accumulated, one after the other one, as compared with a wild type strain. Fig. 7C shows the phenotype of cells grown in

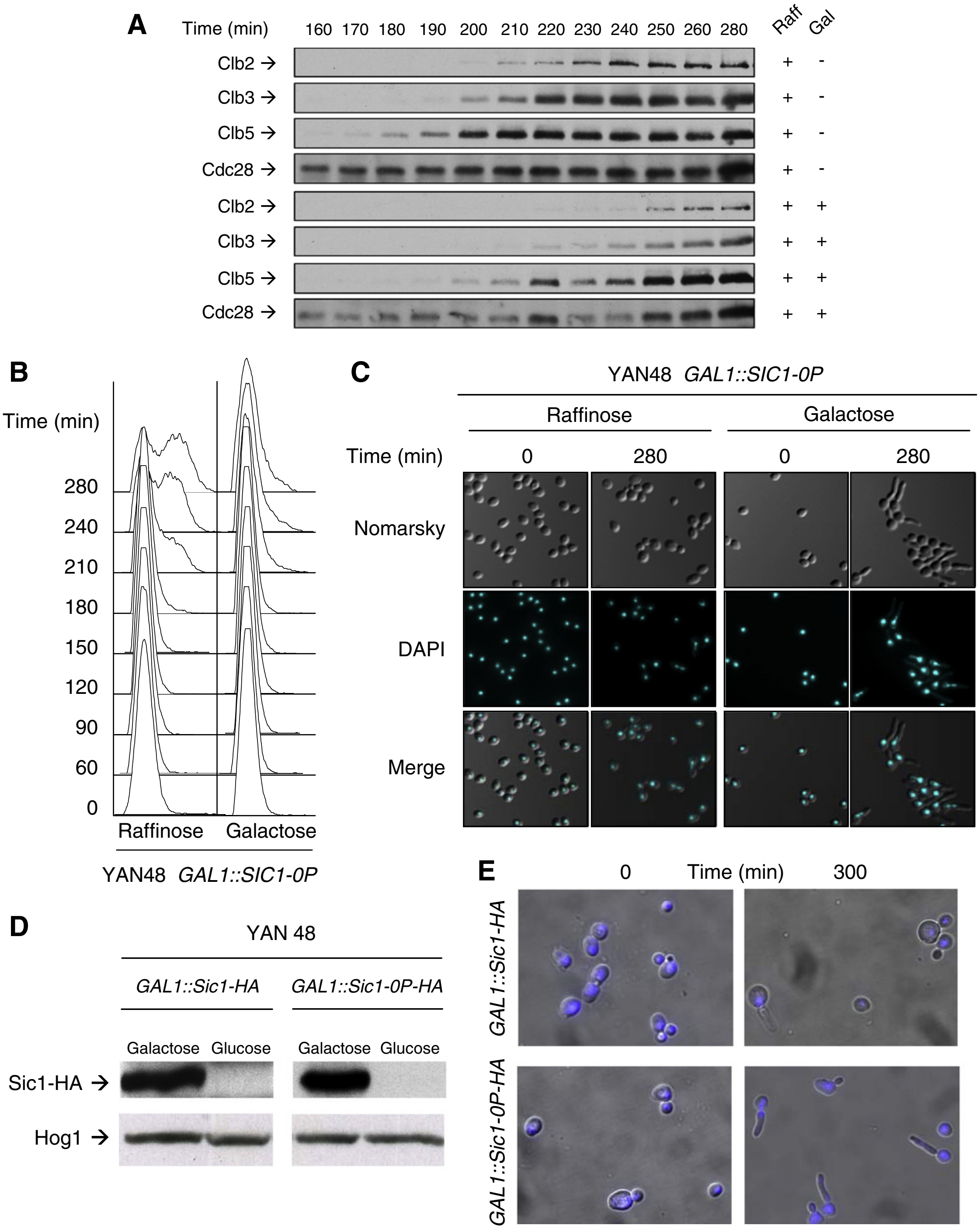

Fig. 7. Over-expression of *SIC1-0P* exacerbates the difference in onset of Clbs waves. (A) Time course of Clb2, Clb3 and Clb5 onset. Newborn YAN48 cells over-expressing *SIC1-0P* were recovered from elutriation and grown in SD medium plus 2% raffinose in presence or absence of 1% galactose. Samples were taken at the indicated times to be analysed by Western blot. (B) Cell synchrony. The same time points reported in (A) were sampled to measure both DNA content by Flow Cytometry. (C) Abnormal bud formation in *SIC1-0P* expressing cells. The same cells reported in (A) were sampled after elutriation (time = 0) and at the end of experiment (time = 280), fixed and treated with DAPI to visualize DNA along with Nomarsky contrast filter. (D) Wild type Sic1-HA and Sic1-0P-HA proteins were revealed by Western blot anti-HA, showing the same level of expression. Hog1 was detected as a loading control. (E) Morphology of *SIC1* and *SIC1-0P* expressing cells. Yeast cells were grown overnight on raffinose medium lacking uracil, resuspended on either glucose or galactose containing media, then incubated at 30 °C for 5 h, fixed and stained with DAPI for visualization.

raffinose or in raffinose plus galactose media immediately after elutriation (0 min) and at the end of the time course experiment (280 min). In the condition raffinose plus galactose, abnormal bud formation is observed (280 min), clearly indication of *SIC1-0P* expression. Being a stronger antagonist of the Cdk1-Clb activity, a non-degradable variant of Sic1 is expected to produce a defective cellular phenotype as compared to Sic1 over-expression, which instead inhibits cell cycle progression only of a subset of cells in the yeast population, as reported (Nugroho and Mendenhall, 1994). The level of over-expression of galactose-induced wild type *SIC1* and *SIC1-0P* is similar (Fig. 7D), however the effect on cellular morphology is remarkably different. In fact, about 15% of cells over-expressing a wild type *SIC1* show an elongated morphology – in agreement with the range 10–25% reported by Nugroho and Mendenhall –whereas inducing *SIC1-0P* the percentage increases to about 60% (Fig. 7E). This demonstrates that the effect observed is not due to Sic1 over-expression and suggests that defects in cell division observed in Sic1-0P could be a consequence of an altered timing of Clb waves.

An increased amount of Sic1 did not impair but delayed the formation of Clbs waves. However, it is difficult to assess whether this is a direct consequence of Sic1 excess on levels of Clbs or a secondary effect due to *SIC1-0P*-dependent delay in cell cycle progression. Therefore, we investigated by computational simulations the possible effect of an artificially non-degradable Sic1 (which mimics the *SIC1-0P* variant) or an over-expressed Sic1 on the formation of Clb waves. Starting from the network shown in Fig. 2G, we considered that Sic1 was artificially over-expressed and not degraded (*SIC1-0P*) by any of Cdk1–Clbs (reaction rates 5, 14 and 18 are set to 0), allowing only its constitutive degradation (reaction 26). Fig. 8A shows the simulation of Clb total levels already presented in Fig. 2H, with an additional curve of Sic1 levels in time. Considering that experimental measurements frequently show only relative changes and, as reported, there is no real agreement on absolute levels for Sic1 as well as for Clbs (Cross et al., 2002; Ghaemmaghami et al., 2003), we normalized concentrations to 1 to get compatible time courses and absolute protein levels were not considered. As observed in Fig. 8B, levels of *SIC1-0P* decreased slowly, and all Clbs raised also slowly, as compared to the time scale (60 min) considered in Fig. 8A. However, by extending the time scale, the successive appearance of Clbs was observed again (Fig. 8C), suggesting that if Sic1 was not regulated for its degradation, possibly the cells would have a much longer G_1 phase. Contrarily, over-expression of a wild type Sic1 (*SIC1*) shows already after 60 min a different slope of both Sic1 decrease and Clb increase, as compared with a not degraded Sic1 (Fig. 8D). Strikingly, by extending the time scale, Clb waves were observed to peak early and in a narrow timing corresponding to Sic1 minimum level and to disappear together in a shaped fashion (Fig. 8E). These results, together with data presented in Fig. 5, suggest that a functional Sic1 might coordinate waves of temporal Clb activity. Moreover, a non-degradable Sic1 seems to have a stronger effect, delaying cell cycle progression due to a different timing of Clb waves, prediction that requires a

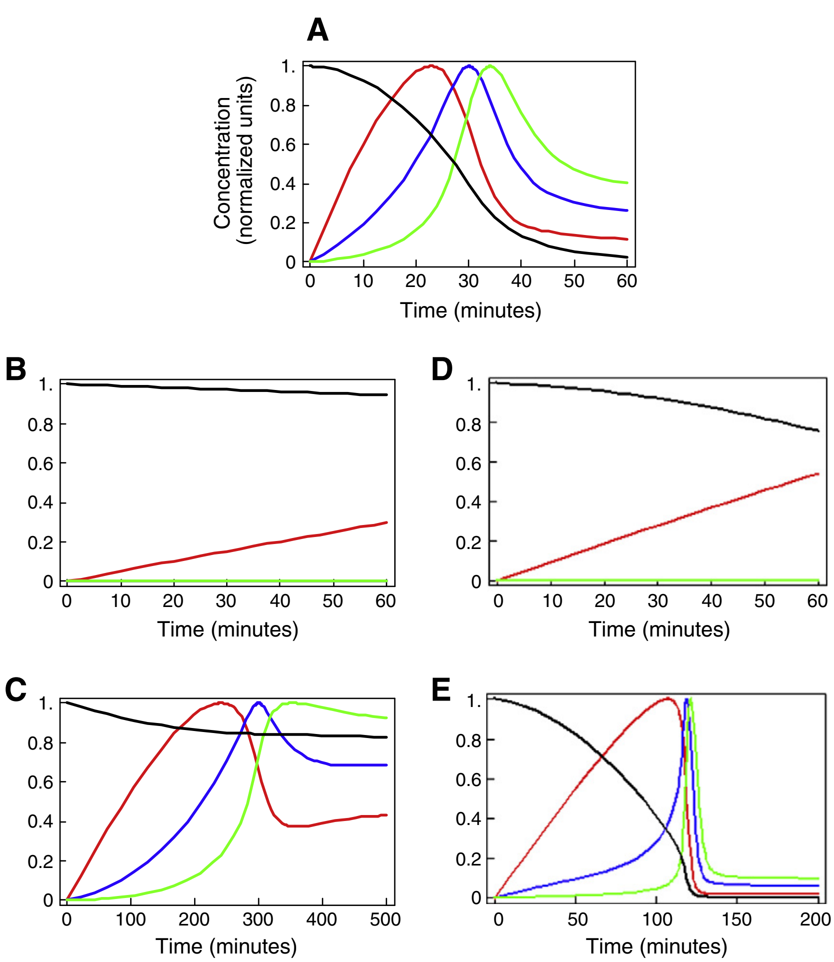

Fig. 8. Simulation of Clb waves after over-expression of *SIC1-0P* and *SIC1*. (A) Simulation showing total levels of wild type Sic1 and Clbs in the network of Fig. 2G. All concentrations are normalized to 1. Protein levels are indicated with different colours: Sic1 in black, Clb5,6 in red, Clb3,4 in blue and Clb1,2 in green. (B) Sic1-0P and Clbs are plotted up to 60 min. (C) Sic1-0P and Clbs are plotted up to 500 min. (D) Over-expressed Sic1 and Clbs are plotted up to 60 min. (E) Over-expressed Sic1 and Clbs are plotted up to 200 min.

new experimental test. This prediction is in line with the fact that cells expressing *SIC1-0P* show a defective phenotype with an increasing elongated morphology, as observed in Fig. 7E.

All together, our findings suggest that Sic1 offers a feed-forward regulation to trigger the waves of Clb levels and the timing of their appearance, therefore contributing to the robustness of the cell cycle.

4. Discussion

The biochemical regulation that controls cell cycle has been recognized to be the oscillation of Cdk1 activity, where Clbs bind to Cdk1 kinase with the characteristic staggered behaviour known as "waves of cyclins" (Fitch et al., 1992; Futcher, 1996; Koch and Nasmyth, 1994). However, to our knowledge, the mechanism of this coordinated regulation remains elusive.

In this work, we suggest a new perspective for the role of Sic1, the Cdk1–Clb inhibitor, in the regulation of waves of Clb levels. The network we proposed in which Sic1 binds to, and regulates the equilibrium of, all Cdk1–Clb complexes reproduced the oscillatory behaviour of Clbs, and experimental data showed the interaction between Sic1 with all Clbs by means of yeast-two-hybrid and GST pull-down analyses. Global sensitivity analysis supported our findings, demonstrating that the results are not critically dependent on the specific parameter choice. Moreover, Sic1 coexists in time with all Clbs and appears to drive their staggering during cell cycle progression. Furthermore, we found that in *sic1Δ* cells, which show a high frequency of chromosome loss and breakage (Nugroho and Mendenhall, 1994), all Clbs accumulate prematurely losing timing and periodicity of their appearance. This finding is supported by the fact that, in this strain, Clb5 accumulates earlier compared to the wild type and generates a too high Cdk1–Clb5,6 activity in G_1, promoting early DNA replication from few origins (Lengronne and Schwob, 2002). Consequently, an uncontrolled pattern of Clb expression can provoke a not complete DNA replication in a timely manner with cells that mis-segregate replicated chromosomes, resulting in extensive chromosome loss. Finally, we showed both experimentally and computationally that overexpression of a non-degradable form of Sic1 (*SIC1-0P*) delays the formation of all Clb waves. Thus, Sic1 could play a critical role in coordinating replication with mitotic events, possibly coordinating the temporal expression of Clbs.

Furthermore, our mathematical analysis confirmed that Clb-regulated degradation is not essential to generate waves of cyclins. Although both cyclin degradation and specificity contribute to the triggering of sequential cell cycle events to generate a robust cell cycle (Bloom and Cross, 2007), they are not an absolute requirement for a viable cell cycle. Moreover, in the case of constitutive Clb expression, waves of Cdk1–Clb activity can be still observed. This is due to the fact that oscillations in Sic1 level are enough to trigger the feed-forward loop necessary for the switching of Cdk1–Clb complexes between states of high and low concentrations (Thornton and Toczyski, 2003). Our results are in agreement with this vision, and propose a role for Sic1 in coordinating the appearance of Cdk1–Clbs, rather than their proteolysis, to regulate cell cycle events.

4.1. Is Sic1 part of the mechanism that regulates cell cycle coordination?

The model here presented can be reduced to a variation of the classical biochemical switch between an inhibitor I (Sic1) and an activator A (Clb) (Fig. 9A). In this view, the scheme follows the typical hybrid feedback loop motif of oscillations found in nature (Tiana et al., 2007), where the double inhibition between I and A_i results in a positive feedback loop on A_i (Fig. 9B).

Our computational finding that an artificially not degraded Sic1 does not impair the formation of Clb waves is supported by recent data showing that yeast cells expressing an unphosphorylatable

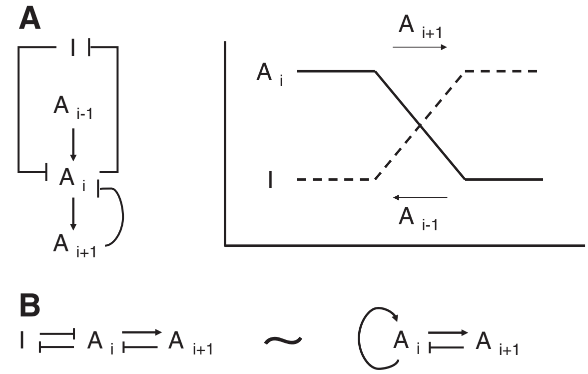

Fig. 9. Negative feedbacks loops of the signalling network. (A) Biochemical switch between an inhibitor I (Sic1) and an activator A (Clb). (B) Hybrid feedback loop motif of natural oscillations. The mutual inhibition between I and A_i results in a positive feedback loop on A_i characteristic for double negative feedback loops. In all figures a normal arrow represents an activating interaction, and a barred arrow represents a repressing interaction.

(non-degradable) form of Sic1 delayed DNA replication due to the postponed activation of the Cdk1-Clb activity (Cross et al., 2007). These data suggest that stable Sic1 transiently blocks Cdk1–Clb activation, but that ultimately the total level of these complexes increases above the Sic1 level. This is in agreement with the finding that cells carrying *SIC1-0P* are lethal in absence of *CLB2*, *CLB3* or *CLB5* genes (Cross et al., 2007). In support to this vision, we have shown that Sic1 directly interacts with all Clbs and *SIC1-0P* over-expression delays the appearance of all Clb waves, reflecting the different activity that Clbs play at various stages in the cell cycle (Cross et al., 2002; Miller and Cross, 2001).

Based on our findings, we argue that Sic1 may be part of the mechanism that coordinates cell cycle regulation. Is an additional function of Sic1 to synchronize waves of Clb levels with other cell cycle processes? Stabilization and destabilization of Sic1 in late stages of the cell cycle still have to be proven, but there is evidence for a possible involvement of kinases and phosphatases in its fine-tuned regulation. Sic1 is targeted at multiple sites by several kinases such as Hog1 (Escote et al., 2004), Pho85 (Nishizawa et al., 1998), Ime2 (Sedgwick et al., 2006) and CK2 (Barberis et al., 2005b; Coccetti et al., 2006), but the effect of these phosphorylations on Sic1 stability is not fully understood. In addition, phosphorylations stabilizing Sic1 has been also reported, mediated by the phosphatase Cdc14 (Visintin et al., 1998) and Dcr2 (Pathak et al., 2007).

5. Conclusion

Biochemical feedback and feed-forward loops commonly serve to coordinate oscillations of cellular processes occurring over a wide range of time scales. Quantitative properties, such as high basal degradation rates of proteins, tend to dampen these oscillations. In the cell cycle of budding yeast, passage through different phases employs multiple specific Cdk1-Clb complexes in a fixed sequence. Clbs bind to Cdk1 kinase with the characteristic staggered behaviour known as "waves of cyclins". In the present study, our combined computational and experimental analyses support the fact that Sic1 may coordinate the staggering of phase-specific Clb levels, generating the characteristic pattern of waves. Moreover, we provide evidence supporting the vision that Clb-regulated degradation is not essential to generate cyclin waves. Future studies will have to concentrate on identifying additional mechanisms, besides Sic1 degradation via Cdk1–Cln and Cdk1–Clb phosphorylations, by which Sic1 can be regulated. This could be investigated on the one side by testing experimentally the involvement of kinases and phosphatases known to play a role in Sic1 regulation, and on the other side by searching for novel regulators of Sic1.

Contributors

MB conceived the biological idea and computational and experimental studies, designed mathematical models and experiments, performed the mathematical analysis. EK helped in the setting of the global sensitivity analysis. MB and CL performed yeast-two-hybrid and GST pull-down experiments. MÀA performed time courses data. MÀA and AG-N performed microscopic analyses. MB, CL, MÀA, AG-N, HL, SK, FP and EK analysed data. MB wrote the manuscript with contribution from SK, FP and EK.

Acknowledgments

We thank Nora Figueras for help in performing part of the cloning in early stages of the research and Simon Borger and Joyce So for critical reading of the manuscript. We also thank Béla Novák for useful criticisms on the mathematical model. This work was supported by grants from the Experimental Resources Funding from ENFIN, a Network of Excellence funded by the European Commission, to MB (within contract number LSHG-CT-2005-518254 to EK). Part of the work was supported by grants from the European Commission (contract number HEALTH-2007-201142, UNICELLSYS) to SK, FP and EK.

Appendix A

Ordinary differential equations (ODEs) of the networks describing the dynamics of Cdk1–Clb activation are listed as follows.

Network Fig. 2

$$\frac{d[Sic1]}{dt} = -k_2[Sic1]\times[Cdk1\cdot Clb5,6] + k_3[Cdk1\cdot Clb5,6\cdot Sic1] - k_{11}[Sic1]\times[Cdk1\cdot Clb1,2] + k_{12}[Cdk1\cdot Clb1,2\cdot Sic1] - k_{15}[Sic1]\times[Cdk1\cdot Clb3,4] + k_{16}[Cdk1\cdot Clb3,4\cdot Sic1] - k_{26}[Sic1] \quad (A.1.1)$$

$$\frac{d[Cdk1\cdot Clb5,6]}{dt} = k_1 - k_2[Sic1]\times[Cdk1\cdot Clb5,6] + k_3[Cdk1\cdot Clb5,6\cdot Sic1] + k_5[Cdk1\cdot Clb5,6\cdot Sic1]\times(1+[Cdk1\cdot Clb5,6] + [Cdk1\cdot Clb3,4] + [Cdk1\cdot Clb1,2]) + -k_6[Cdk1\cdot Clb5,6] \quad (A.1.2)$$

$$\frac{d[Cdk1\cdot Clb5,6\cdot Sic1]}{dt} = k_2[Sic1]\times[Cdk1\cdot Clb5,6] - k_3[Cdk1\cdot Clb5,Sic1] - k_5[Cdk1\cdot Clb5,6\cdot Sic1]\times(1+[Cdk1\cdot Clb5,6]+[Cdk1\cdot Clb3,4] + [Cdk1\cdot Clb1,2]) - K_4[Cdk1\cdot Clb5,6\cdot Sic1] \quad (A.1.3)$$

$$\frac{d[Sic1degr1]}{dt} = k_5[Cdk1\cdot Clb5,6\cdot Sic1]\times(1+[Cdk1\cdot Clb5,6]+[Cdk1\cdot Clb3,4] + [Cdk1\cdot Clb1,2]) \quad (A.1.4)$$

$$\frac{d[Clb5,6\ degr]}{dt} = k_4[Cdk1\cdot Clb5,6\cdot Sic1] + k_6[Cdk1\cdot Clb5,6] \quad (A.1.5)$$

$$\frac{d[Cdk1\cdot Clb3,4]}{dt} = k_7(1+k_A[Cdk1\cdot Clb5,6]) - k_{15}[Sic1]\times[Cdk1\cdot Clb3,4] + k_{16}[Cdk1\cdot Clb3,4\cdot Sic1] - k_8[Cdk1\cdot Clb3,4] \quad (A.1.6)$$

$$\frac{d[Cdk1\cdot Clb3,4\cdot Sic1]}{dt} = k_{15}[Sic1]\times[Cdk1\cdot Clb3,4] - k_{16}[Cdk1\cdot Clb3,4\cdot Sic1] - k_{18}[Cdk1\cdot Clb3,4\cdot Sic1]\times(1+[Cdk1\cdot Clb5,6]+[Cdk1\cdot Clb3,4] + [Cdk1\cdot Clb1,2]) + -k_{17}[Cdk1\cdot Clb3,4\cdot Sic1] \quad (A.1.7)$$

$$\frac{d[Sic1degr2]}{dt} = k_{18}[Cdk1\cdot Clb3,4\cdot Sic1]\times(1+[Cdk1\cdot Clb5,6]+[Cdk1\cdot Clb3,4] + [Cdk1\cdot Clb1,2]) \quad (A.1.8)$$

$$\frac{d[Clb3,4\ degr]}{dt} = k_{17}[Cdk1\cdot Clb3,4\cdot Sic1] + k_8[Cdk1\cdot Clb3,4] \quad (A.1.9)$$

$$\frac{d[Cdk1\cdot Clb1,2]}{dt} = k_9(1+k_D[Cdk1\cdot Clb1,2] + k_B[Cdk1\cdot Clb3,4] + k_C[Cdk1\cdot Clb5,6]) - k_{11}[Sic1]\times[Cdk1\cdot Clb1,2] + k_{12}[Cdk1\cdot Clb1,2\cdot Sic1] - k_{10}[Cdk1\cdot Clb1,2] \quad (A.1.10)$$

$$\frac{d[Cdk1\cdot Clb1,2\cdot Sic1]}{dt} = k_{11}[Sic1]\times[Cdk1\cdot Clb1,2] - k_{12}[Cdk1\cdot Clb1,2\cdot Sic1] - k_{14}[Cdk1\cdot Clb1,2\cdot Sic1]\times(1+[Cdk1\cdot Clb5,6]+[Cdk1\cdot Clb3,4] + [Cdk1\cdot Clb1,2]) - k_{13}[Cdk1\cdot Clb1,2\cdot Sic1] \quad (A.1.11)$$

$$\frac{d[Sic1\ degr3]}{dt} = k_{14}[Cdk1\cdot Clb1,2\cdot Sic1]\times(1+[Cdk1\cdot Clb5,6]+[Cdk1\cdot Clb3,4] + [Cdk1\cdot Clb1,2]) \quad (A.1.12)$$

$$\frac{d[Clb1,2\,degr]}{dt} = k_{13}[Cdk1\cdot Clb1,2\cdot Sic1] + k_{10}[Cdk1\cdot Clb1,2] \quad (A.1.13)$$

Network Fig. B.9

A.2.1–A.2.5 equal to A.1.1–A.1.5 (Network Fig. 2).

$$\frac{d[Cdk1\cdot Clb3,4]}{dt} = k_{21}[Cdk1]\times[Clb3,4] - k_{22}[Cdk1\cdot Clb3,4] - k_{15}[Sic1]\times[Cdk1\cdot Clb3,4] + k_{16}[Cdk1\cdot Clb3,4\cdot Sic1] - k_8[Cdk1\cdot Clb3,4] \quad (A.2.6)$$

A.2.7–A.2.9 equal to A.1.7–A.1.9 (Network Fig. 2).

$$\frac{d[Cdk1\cdot Clb1,2]}{dt} = k_{24}[Cdk1]\times[Clb1,2] - k_{25}[Cdk1\cdot Clb1,2] - k_{11}[Sic1]\times[Cdk1\cdot Clb1,2] + k_{12}[Cdk1\cdot Clb1,2\cdot Sic1] - k_{10}[Cdk1\cdot Clb1,2] \quad (A.2.10)$$

A.2.11–A.2.13 equal to A.1.11–A.1.13 (Network Fig. 2).

$$\frac{d[mRNACLB3,4]}{dt} = k_7(1+k_A[Cdk1\cdot Clb5,6]) - k_{19}[mRNACLB3,4] \quad (A.2.14)$$

$$\frac{d[Clb3,4]}{dt} = k_{19}[mRNACLB3,4] - k_{21}[Cdk1]\times[Clb3,4] + k_{22}[Cdk1\cdot Clb3,4] \quad (A.2.15)$$

$$\frac{d[Cdk1]}{dt} = k_{20} - k_{21}[Cdk1]\times[Clb3,4] + k_{22}[Cdk1\cdot Clb3,4] - k_{24}[Cdk1]\times[Clb1,2] + k_{25}[Cdk1\cdot Clb1,2] \quad (A.2.16)$$

$$\frac{d[mRNACLB1,2]}{dt} = k_9(1 + k_D[Cdk1\cdot Clb1,2] + k_B[Cdk1\cdot Clb3,4] + k_C[Cdk1\cdot Clb5,6]) - k_{23}[mRNACLB1,2] \quad (A.2.17)$$

$$\frac{d[Clb1,2]}{dt} = k_{23}[mRNACLB1,2] - k_{24}[Cdk1]\times[Clb1,2] + k_{25}[Cdk1\cdot Clb1,2] \quad (A.2.18)$$

Network Fig. 6

A.3.1 equal to A.1.1 (Network Fig. 2).

$$\frac{d[Cdk1\cdot Clb5,6]}{dt} = k_1 - k_2[Sic1]\times[Cdk1\cdot Clb5,6] + k_3[Cdk1\cdot Clb5,6\cdot Sic1] + k_5[Cdk1\cdot Clb5,6\cdot Sic1]\times(1 + [Cdk1\cdot Clb5,6] + [Cdk1\cdot Clb3,4] + [Cdk1\cdot Clb1,2]) - k_6[Cdk1\cdot Clb5,6] \times(1 + k_E[Cdk1\cdot Clb3,4] + k_F[Cdk1\cdot Clb1,2]) \quad (A.3.2)$$

A.3.3–A.3.4 equal to A.1.3–A.1.4 (Network Fig. 2).

$$\frac{d[Clb5,6\,degr]}{dt} = k_4[Cdk1\cdot Clb5,6\cdot Sic1] + k_6[Cdk1\cdot Clb5,6] \times(1 + k_E[Cdk1\cdot Clb3,4] + k_F[Cdk1\cdot Clb1,2]) \quad (A.3.5)$$

$$\frac{d[Cdk1\cdot Clb3,4]}{dt} = k_7(1 + k_A[Cdk1\cdot Clb5,6]) - k_{15}[Sic1]\times[Cdk1\cdot Clb3,4] + k_{16}[Cdk1\cdot Clb3,4\cdot Sic1] - k_8[Cdk1\cdot Clb3,4] \times(1 + k_G[Cdk1\cdot Clb1,2]) \quad (A.3.6)$$

A.3.7–3.8 equal to A.2.7–A.2.8 (Network Fig. 2).

$$\frac{d[Clb3,4\,degr]}{dt} = k_{17}[Cdk1\cdot Clb3,4\cdot Sic1] + k_8[Cdk1\cdot Clb3,4] \times(1 + k_G[Cdk1\cdot Clb1,2]) \quad (A.3.9)$$

$$\frac{d[Cdk1\cdot Clb1,2]}{dt} = k_9(1 + k_D[Cdk1\cdot Clb1,2] + k_B[Cdk1\cdot Clb3,4] + k_C[Cdk1\cdot Clb5,6]) - k_{11}[Sic1]\times[Cdk1\cdot Clb1,2] + k_{12}[Cdk1\cdot Clb1,2\cdot Sic1] - k_{10}[Cdk1\cdot Clb1,2] \times(1 + k_H[Cdk1\cdot Clb1,2]) \quad (A.3.10)$$

A.3.11–A.3.12 equal to A.1.11–A.1.12 (Network Fig. 2).

$$\frac{d[Clb1,2\,degr]}{dt} = k_{13}[Cdk1\cdot Clb1,2\cdot Sic1] + k_{10}[Cdk1\cdot Clb1,2] \times(1 + k_H[Cdk1\cdot Clb1,2]) \quad (A.3.13)$$

In the analyses, the biochemical reactions are described by means of mass action kinetics. However, the regulation of transcription might be strongly non-linear and threshold-like, rather than linear as considered here. If Cdk1–Clb3,4 is required for priming *CLB1,2*, and *CLB1,2* genes are only triggered after a large amount of Cdk1–Clb5,6 has passed, this could generate a delay in the absence of Sic1 regulation of Cdk1–Clb3,4. In order to test this hypothesis, the activation of Cdk1–Clb by Michaelis–Menten equations was modelled (unpublished data). The simulations did not reproduce the wave-like behaviour that we obtained using mass action kinetics. Mass action kinetics can be used as a reasonable description of the condensed and highly simplified transcriptional regulation processes considered here.

Table A.1
Parameters of networks describing dynamics of Cdk1-Clb activation. The initial concentration of Sic1 is set to 5 in all simulations, whereas initial concentrations of the other components are set to zero. Concentrations are given in dimensionless units.

Network Fig. 2		Network Fig. B.9		Network Fig. 6	
$k_1=0.1$	$k_{18}=0.05$	$k_1=0.1$	$k_{18}=0.05$	$k_1=0.1$	$k_{18}=0.05$
$k_2=5$		$k_2=5$	$k_{19}=1$	$k_2=5$	
$k_3=0.5$		$k_3=0.5$	$k_{20}=1$	$k_3=0.5$	
$k_4=0.01$		$k_4=0.01$	$k_{21}=5$	$k_4=0.01$	
$k_5=0.05$		$k_5=0.05$	$k_{22}=0.5$	$k_5=0.05$	
$k_6=0.7$		$k_6=0.7$	$k_{23}=1$	$k_6=0.7$	
$k_7=0.01$		$k_7=0.01$	$k_{24}=5$	$k_7=0.01$	
$k_8=0.7$		$k_8=0.7$	$k_{25}=0.5$	$k_8=0.7$	
$k_9=0.001$	$k_{26}=0.001$	$k_9=0.001$	$k_{26}=0.001$	$k_9=0.001$	$k_{26}=0.001$
$k_{10}=0.7$	$k_A=100$	$k_{10}=0.7$	$k_A=100$	$k_{10}=0.7$	$k_A=100$
$k_{11}=5$	$k_B=1000$	$k_{11}=5$	$k_B=1000$	$k_{11}=5$	$k_B=1000$
$k_{12}=0.5$	$k_C=100$	$k_{12}=0.5$	$k_C=100$	$k_{12}=0.5$	$k_C=100$
$k_{13}=0.01$	$k_D=100$	$k_{13}=0.01$	$k_D=100$	$k_{13}=0.01$	$k_D=100$
$k_{14}=0.05$		$k_{14}=0.05$		$k_{14}=0.05$	$k_E=1$
$k_{15}=5$		$k_{15}=5$		$k_{15}=5$	$k_F=1$
$k_{16}=0.5$		$k_{16}=0.5$		$k_{16}=0.5$	$k_G=1$
$k_{17}=0.01$		$k_{17}=0.01$		$k_{17}=0.01$	$k_H=1$

Table A.2
Oligonucleotide primers. Underlined primer sequences indicate the restriction sites.

Primer name	Sequence
GST pull-down	
F1_S1myc	5′-CAAGCCAAAGGCATTGTTTCAATCTAGGG ATCAAGAGCATTCTAGAGGTGAACAAAAG-3′
R1_S1myc	5′-TAAAATATAATCGTTCCAGAAACTTTTTTT TTTCATTTCTTAGTGGATCTGATATCATCG-3′
Yeast-two-hybrid	
sic1_FSI	5′-TACAGTCGACAATGACTCCTTCCACC-3′
sic1_RNI	5′-ATTGCGGCCGCTTCAATGCTCTTGATC-3′
clb1_FSI	5′-GCTTGTCGACTAATCTTCTCATAATG-3′
clb1_RNI	5′-ATTGCGGCCGCTTCACTCATGCAATG-3′
clb2_FSI	5′-CAGTCGACATTGATCTTATAGATGTCC-3′
clb2_RNI	5′-ATTGCGGCCGCTTCTCATTCATGCAAGG-3′
clb3_FSI	5′-CTGAGTCGACAATGCATCATAACTCAC-3′
clb3_RNI	5′-TATGCGGCCGCTTTAGTTAGATCTTTC-3′
clb4_FSI	5′-GATAGTCGACACAGATGATGCTTGAAG-3′
clb4_RNI	5′-GAAGCGGCCGCAAGATGAGTAAGTTAG-3′
clb5_FSI	5′-GTAAGTCGACAACAATGGGAGAGAAC-3′
clb5_RNI	5′-GTAGCGGCCGCATTACTAGTACTAATC-3′
clb6_FS1	5′-GCATGTCGACTAAAATGAATTGTATC-3′
clb6_RN1	5′-TATGCGGCCGCTGATCTATGTTTCAAC-3′

Table A.3
Corresponding time (in min) at the maximum peak of Clb concentrations for different networks. The time delay between the peaks within each network is also reported.

Network Fig. 2G	Network Fig. B.9G	Network Fig. 6G
Time (Clb5,6 max level)	Time (Clb5,6 max level)	Time (Clb5,6 max level)
$t_{5,6}=22.88$	$t_{5,6}=23.51$	$t_{5,6}=22.55$
Time (Clb3,4 max level)	Time (Clb3,4 max level)	Time (Clb3,4 max level)
$t_{3,4}=30.06$	$t_{3,4}=31.99$	$t_{3,4}=28.84$
Time (Clb1,2 max level)	Time (Clb1,2 max level)	Time (Clb1,2 max level)
$t_{1,2}=34.06$	$t_{1,2}=37.61$	$t_{1,2}=32.55$
$\Delta\ (t_{3,4}-t_{5,6})=7.18$	$\Delta\ (t_{3,4}-t_{5,6})=8.48$	$\Delta\ (t_{3,4}-t_{5,6})=6.29$
$\Delta\ (t_{1,2}-t_{3,4})=4.00$	$\Delta\ (t_{1,2}-t_{3,4})=5.62$	$\Delta\ (t_{1,2}-t_{3,4})=3.71$
$\Delta\ (t_{1,2}-t_{5,6})=11.18$	$\Delta\ (t_{1,2}-t_{5,6})=14.20$	$\Delta\ (t_{1,2}-t_{5,6})=10.00$

Appendix B

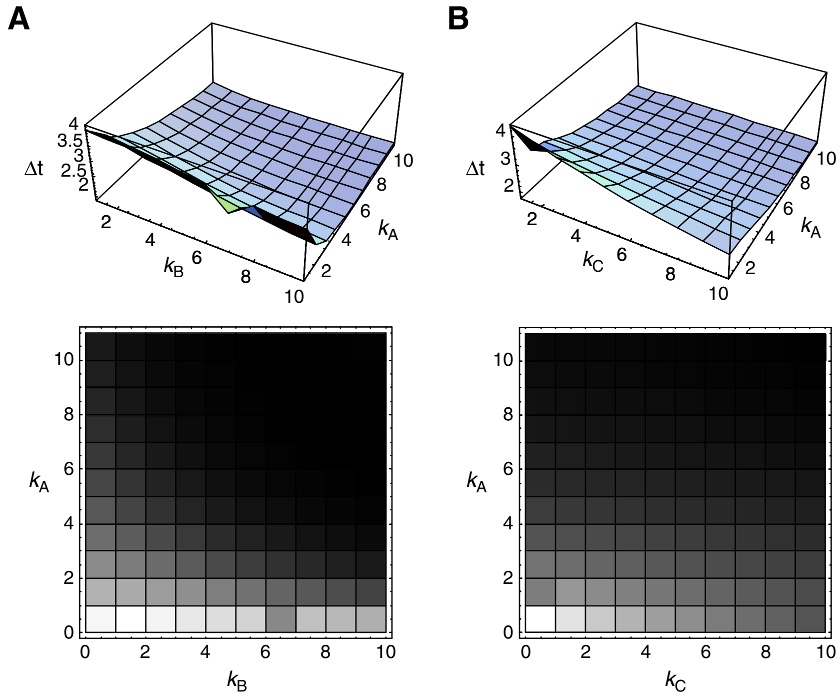

Fig. B.1. Impact of k_A, k_B and k_C on the time delay between time delays of Clb3,4 and Clb1,2. (A) Graph reporting the combination of different values for k_A and k_B is shown together with a 2D visualization. For clarification purposes, the minimum value on the graph (equal to 1, not displayed) corresponds to the minimum value of k_A (50) and k_B (500), while the maximum value on the graph (equal to 10) corresponds to the maximum value of k_A (500) and k_B (5000). (B) Graph reporting the combination of different values for k_A and k_C is shown together with a 2D visualization. For the sake of the clarification, the minimum value on the graph (equal to 1, not displayed) corresponds to the minimum value of both k_A and k_C (50), while the maximum value on the graph (equal to 10) corresponds to the maximum value of both k_A and k_C (500).

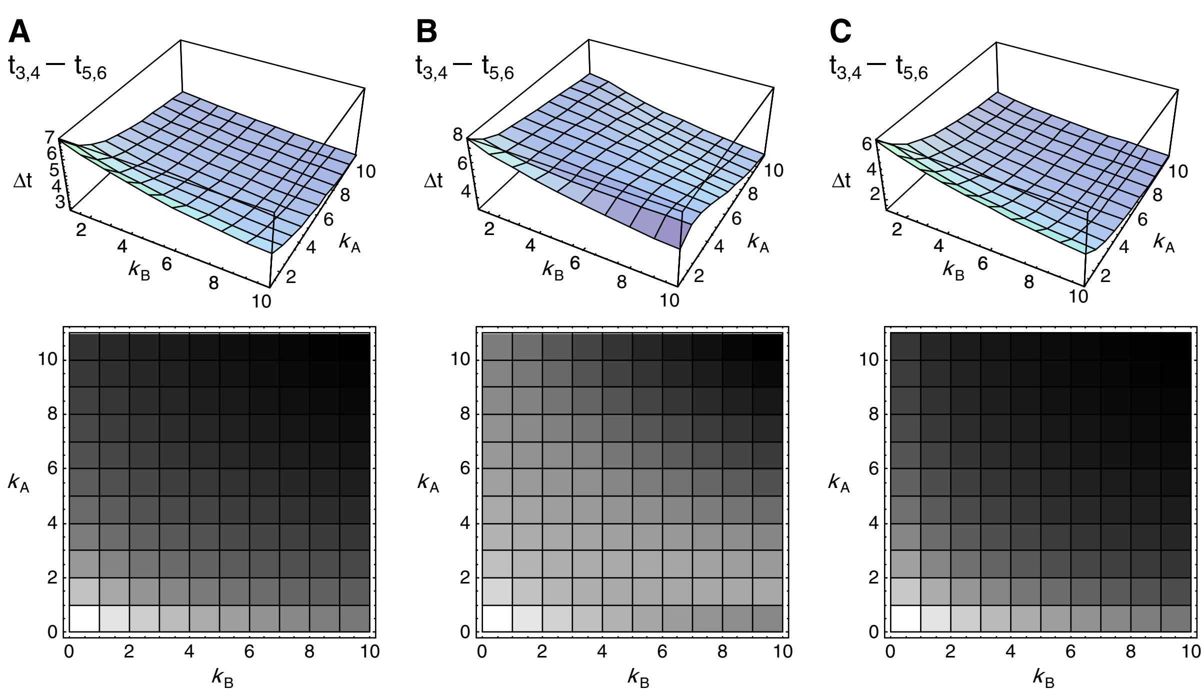

Figs. B.2–B.7. Impact of k_A and k_B or k_A and k_C on the time delay between B-type cyclins. The graphs report a combination of different values of k_A and k_B or k_A and k_C for the three networks under investigation, to obtain the minimum or maximum delay between Clbs. The 2D visualization of the graphs is also shown. For each analysis, panels A, B and C represent simulations for the networks depicted in Figs. 2, B.9 and 6, respectively: $t_{3,4}$–$t_{5,6}$, time delay between Clb5,6 and Clb3,4 (Figs. B.2 and B.5), $t_{1,2}$–$t_{3,4}$, time delay between Clb3,4 and Clb1,2 (Figs. B.3 and B.6); $t_{1,2}$–$t_{5,6}$, time delay between Clb5,6 and Clb1,2 (Figs. B.4 and B.7). The range of values for k_A, k_B and k_C and the graphic interpretations are the same reported in Fig. B.1.

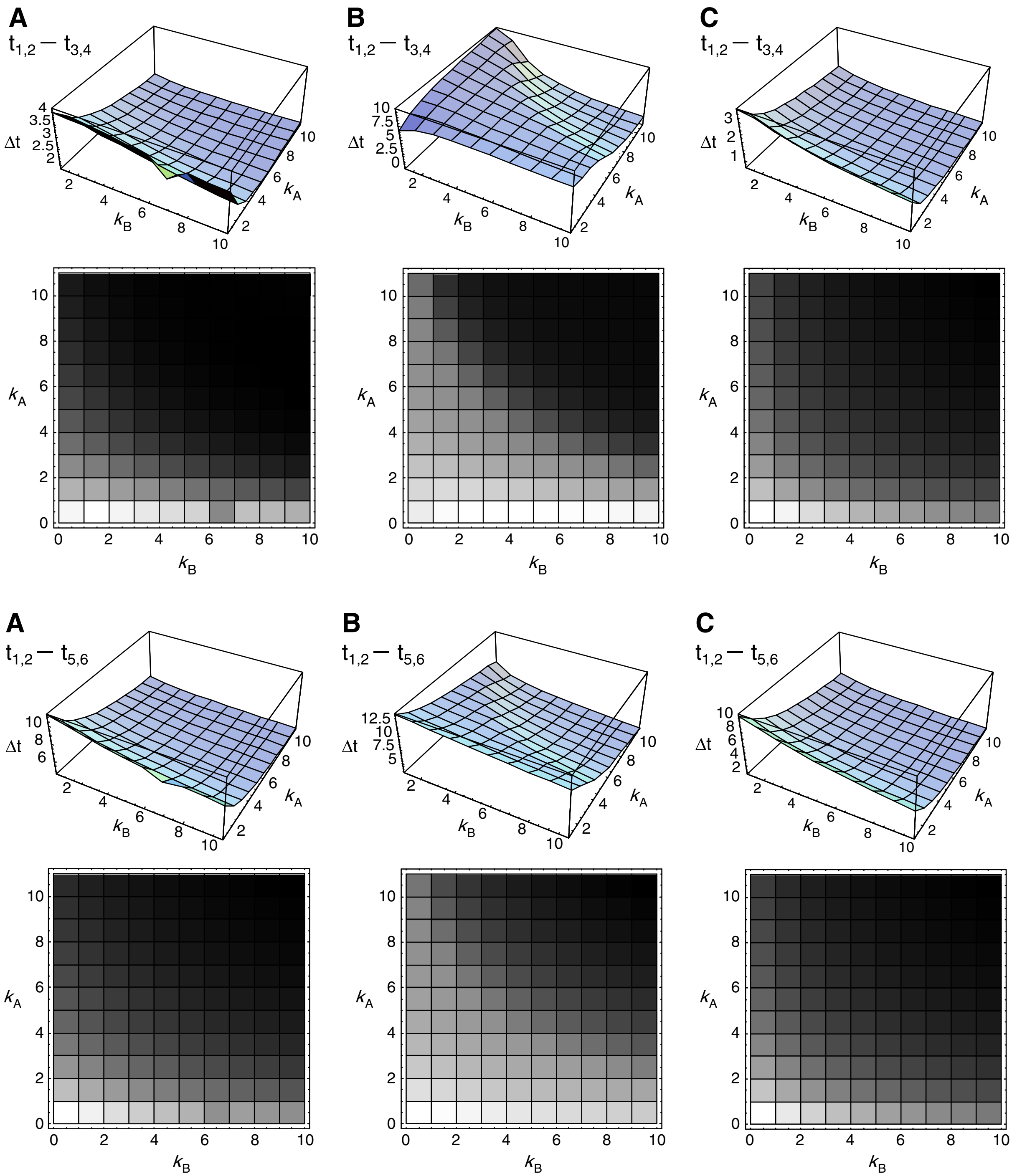

Figs. B.2–B.7 (*continued*).

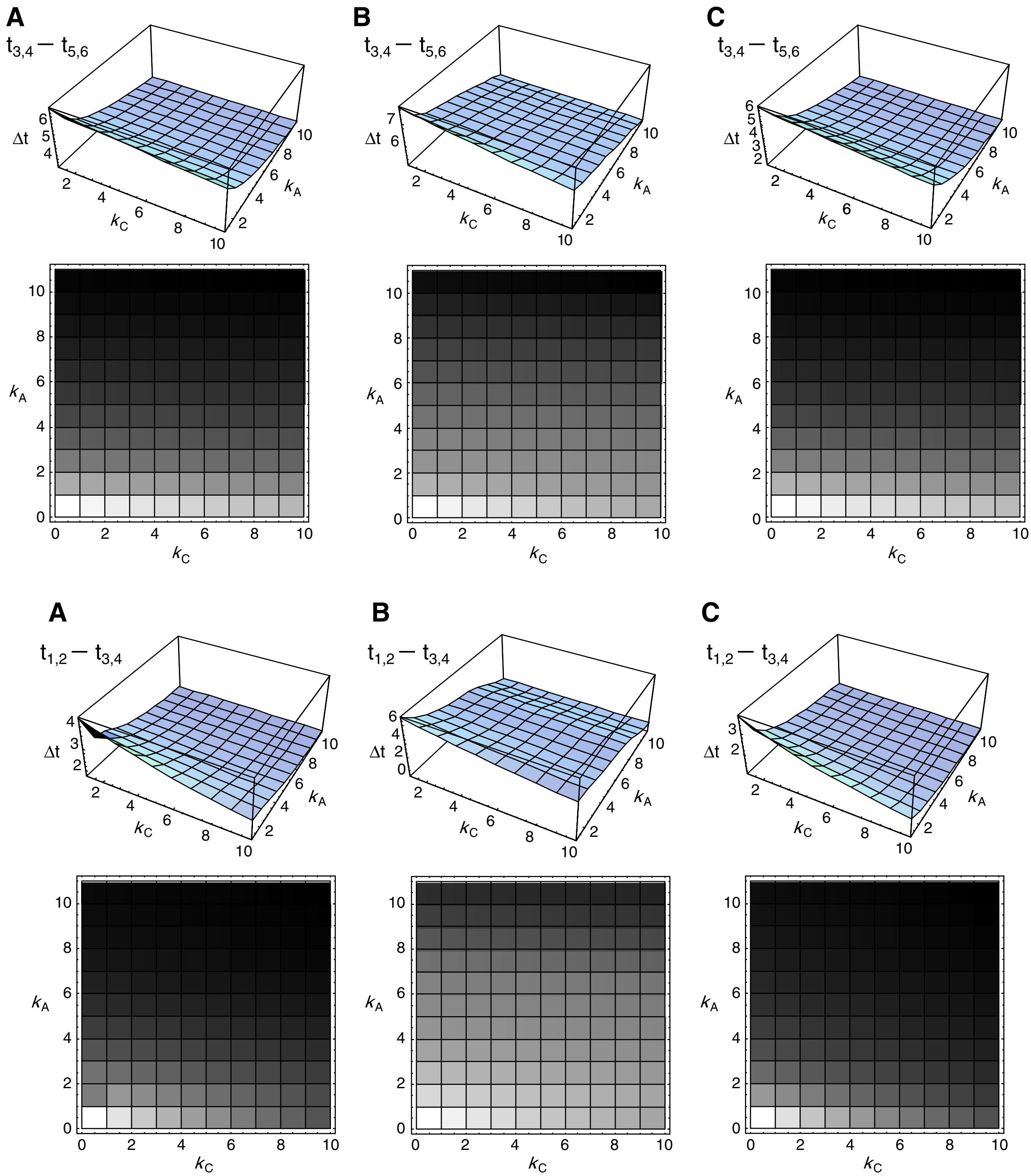

Figs. B.2–B.7 (*continued*).

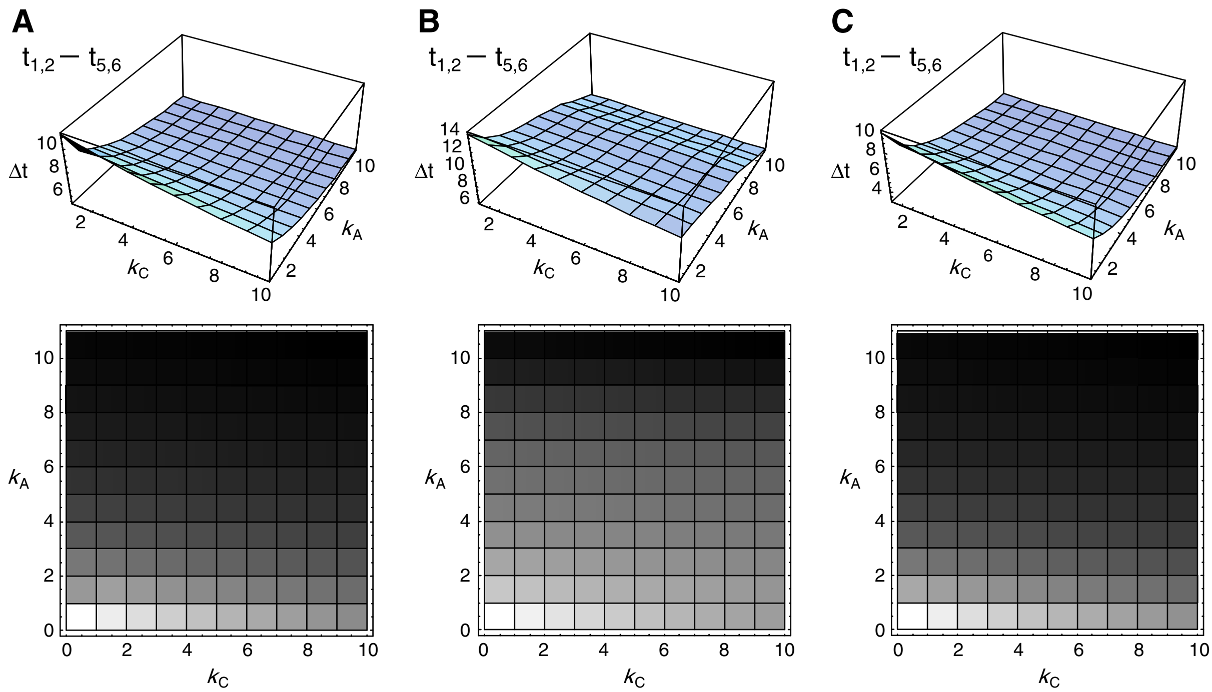

Figs. B.2–B.7 (*continued*).

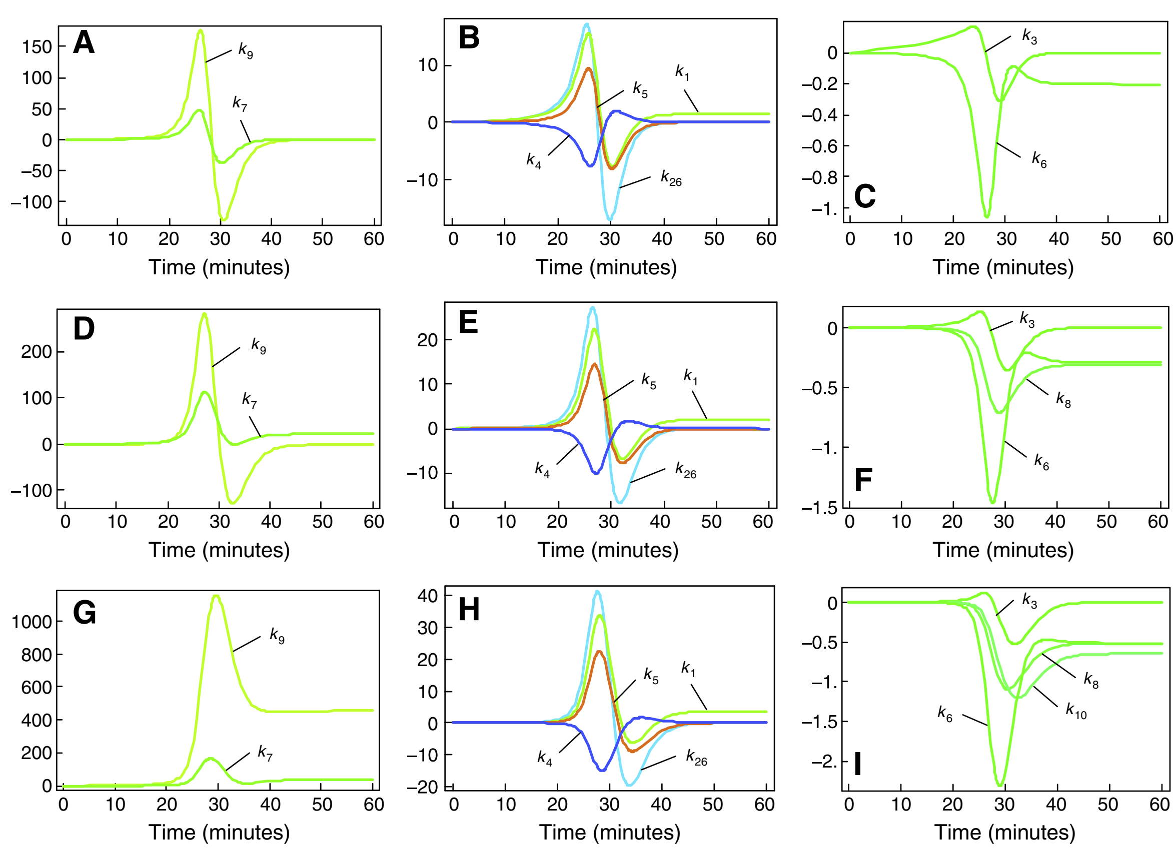

Fig. B.8. Sensitivity analysis of the model in Fig. 2G. Each curve represents the relative change of a concentration time course $c[t]$ caused by an infinitesimal increase in the parameter k ($\partial c[t]/\partial k$). (A–C) Time-dependent response coefficients for Cdk1–Clb5,6. (D–F) Time-dependent response coefficients for Cdk1–Clb3,4. (G–I) Time-dependent response coefficients for Cdk1–Clb1,2.

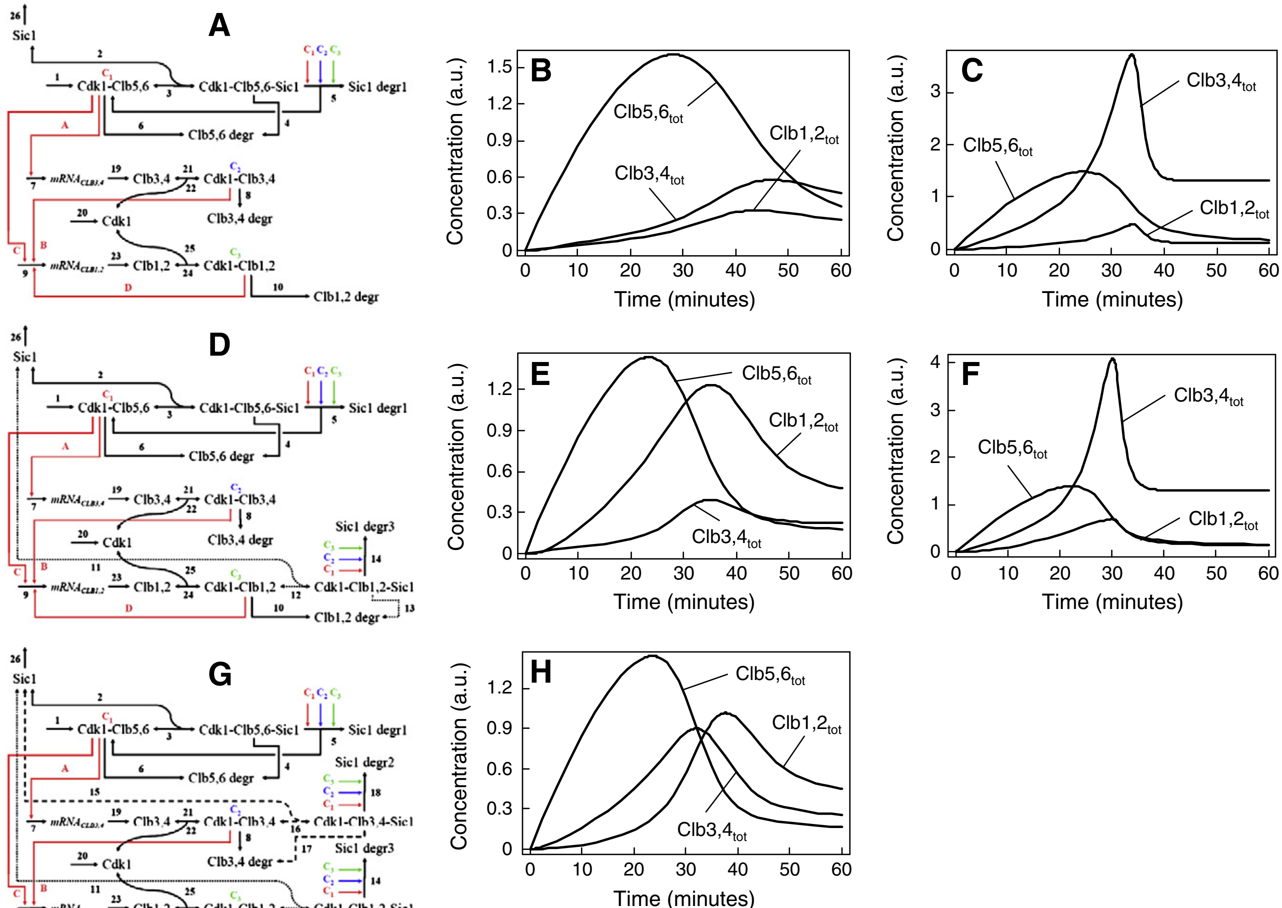

Fig. B.9. Signalling network including steps of Cdk1-Clb formation and computational time courses of total levels of Clb5,6, Clb3,4 and Clb1,2. (A) Network describing the binding of Sic1 to Cdk1–Clb5,6 (solid lines), based on the network shown in Fig. 2A. The additional reactions introduced are: i) when Sic1 is degraded (k_5), Cdk1–Clb5,6 promotes *CLB3,4* mRNA activation (k_A); ii) when Clb3,4 are produced from their mRNAs (k_{19}), they bind to Cdk1 – produced at a constitute level (k_{20}) – forming the Cdk1–Clb3,4 complex (k_{21}); (iii) Cdk1–Clb3,4 in turn promote *CLB1,2* mRNA activation (k_B) together with Cdk1–Clb5,6 (k_C); (iv) when Clb1,2 are produced from their mRNAs (k_{23}), they bind to Cdk1 forming the Cdk1–Clb1,2 complex (k_{24}); (v) Cdk1dissociation from binary complexes (k_{22} and k_{25}) is also considered. The sequential transcriptional activation of Cdk1–Clb complexes is shown in red (k_A, k_B, k_C and k_D). Simulations are carried out with standard values (B) or varying k_A, k_B and k_C (C), as described in the text relative to Fig. 2. (D) Network describing the binding of Sic1 to both Cdk1–Clb5,6 and Cdk1–Clb1,2 (dotted lines). Simulations are carried out with standard values (E) or varying k_A, k_B and k_C (F). (G) Network describing the binding of Sic1 to Cdk1–Clb5,6, Cdk1–Clb1,2 and Cdk1–Clb3,4 (dashed lines). Simulations are carried out with standard values (H). In all simulations, the initial concentration of Sic1 is set to 5, whereas all other initial concentrations are set to 0.

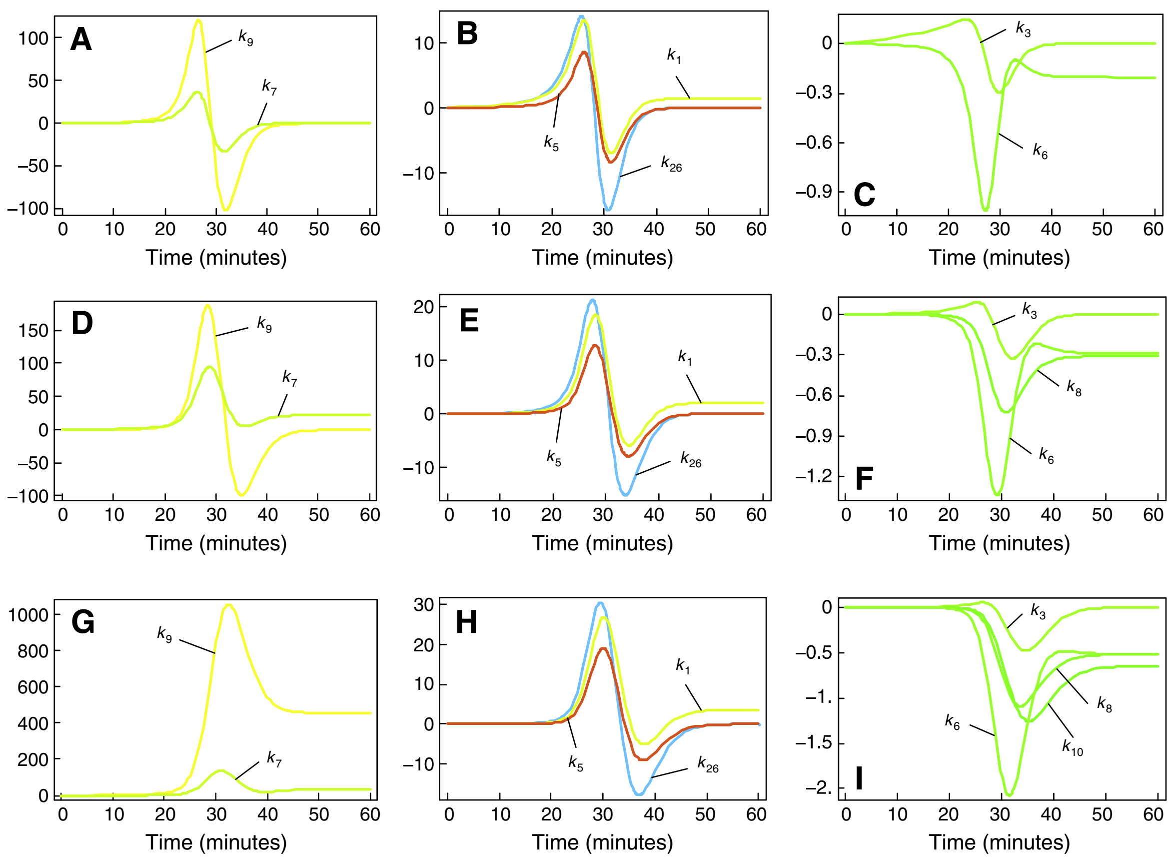

Fig. B.10. Sensitivity analysis of the model in Fig. B.9. The analysis in form of time-dependent response coefficients has been performed as shown in Fig. B.8. (A–C) Time-dependent response coefficients for Cdk1–Clb5,6. (D–F) Time-dependent response coefficients for Cdk1–Clb3,4. (G–I) Time-dependent response coefficients for Cdk1–Clb1,2.

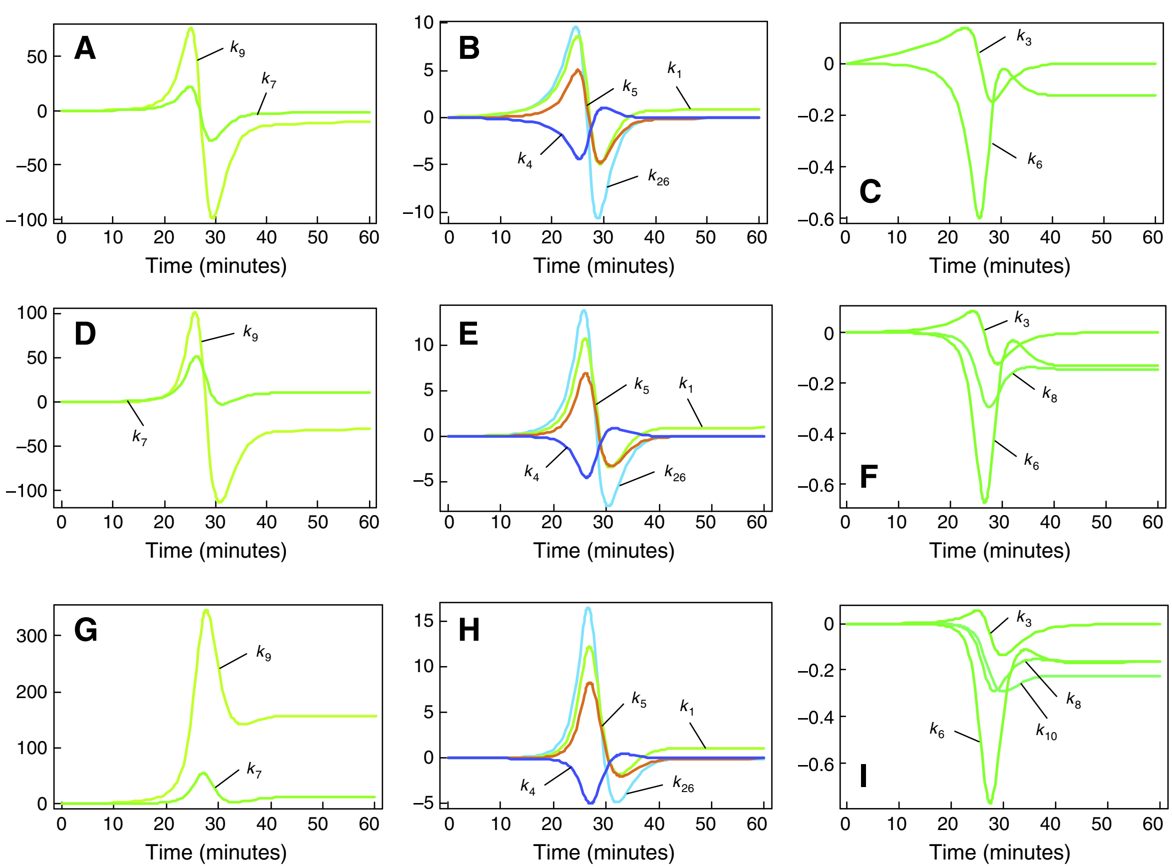

Fig. B.11. Sensitivity analysis of the model in Fig. 6. The analysis in form of time-dependent response coefficients has been performed as shown in Fig. B.8. (A–C) Time-dependent response coefficients for Cdk1–Clb5,6. (D–F) Time-dependent response coefficients for Cdk1–Clb3,4. (G–I) Time-dependent response coefficients for Cdk1–Clb1,2.

References

Aerne BL, Johnson AL, Toyn JH, Johnston LH. Swi5 controls a novel wave of cyclin synthesis in late mitosis. Mol Biol Cell 1998;9:945–56.

Alfieri R, Merelli I, Mosca E, Milanesi L. A data integration approach for cell cycle analysis oriented to model simulation in systems biology. BMC Syst Biol 2007;1:35.

Amon A, Irniger S, Nasmyth K. Closing the cell cycle circle in yeast: G2 cyclin proteolysis initiated at mitosis persists until the activation of G1 cyclins in the next cycle. Cell 1994;77:1037–50.

Archambault V, Li CX, Tackett AJ, Wasch R, Chait BT, Rout MP, et al. Genetic and biochemical evaluation of the importance of Cdc6 in regulating mitotic exit. Mol Biol Cell 2003;14:4592–604.

Archambault V, Chang EJ, Drapkin BJ, Cross FR, Chait BT, Rout MP. Targeted proteomic study of the cyclin-Cdk module. Mol Cell 2004;14:699–711.

Bailly E, Reed SI. Functional characterization of rpn3 uncovers a distinct 19S proteasomal subunit requirement for ubiquitin-dependent proteolysis of cell cycle regulatory proteins in budding yeast. Mol Cell Biol 1999;19:6872–90.

Barberis M, Klipp E. Insights into the network controlling the G(1)/S transition in budding yeast. Genome Inform 2007;18:85–99.

Barberis M, De Gioia L, Ruzzene M, Sarno S, Coccetti P, Fantucci P, et al. The yeast cyclin-dependent kinase inhibitor Sic1 and mammalian p27Kip1 are functional homologues with a structurally conserved inhibitory domain. Biochem J 2005a;387:639–47.

Barberis M, Pagano MA, De Gioia L, Marin O, Vanoni M, Pinna LA, et al. CK2 regulates in vitro the activity of the yeast cyclin-dependent kinase inhibitor Sic1. Biochem Biophys Res Commun 2005b;336:1040–8.

Barberis M, Klipp E, Vanoni M, Alberghina L. Cell size at S phase initiation: an emergent property of the G1/S network. PLoS Comput Biol 2007;3:e64.

Bloom J, Cross FR. Multiple levels of cyclin specificity in cell-cycle control. Nat Rev Mol Cell Biol 2007;8:149–60.

Borg M, Mittag T, Pawson T, Tyers M, Forman-Kay JD, Chan HS. Polyelectrostatic interactions of disordered ligands suggest a physical basis for ultrasensitivity. Proc Natl Acad Sci U S A 2007;104:9650–5.

Breitkreutz A, Choi H, Sharom JR, Boucher L, Neduva V, Larsen B, et al. A global protein kinase and phosphatase interaction network in yeast. Science 2010;328:1043–6.

Chen KC, Csikasz-Nagy A, Gyorffy B, Val J, Novak B, Tyson JJ. Kinetic analysis of a molecular model of the budding yeast cell cycle. Mol Biol Cell 2000;11:369–91.

Chen KC, Calzone L, Csikasz-Nagy A, Cross FR, Novak B, Tyson JJ. Integrative analysis of cell cycle control in budding yeast. Mol Biol Cell 2004;15:3841–62.

Coccetti P, Rossi RL, Sternieri F, Porro D, Russo GL, di Fonzo A, et al. Mutations of the CK2 phosphorylation site of Sic1 affect cell size and S-Cdk kinase activity in *Saccharomyces cerevisiae*. Mol Microbiol 2004;51:447–60.

Coccetti P, Zinzalla V, Tedeschi G, Russo GL, Fantinato S, Marin O, et al. Sic1 is phosphorylated by CK2 on Ser201 in budding yeast cells. Biochem Biophys Res Commun 2006;346:786–93.

Collins SR, Kemmeren P, Zhao XC, Greenblatt JF, Spencer F, Holstege FC, et al. Toward a comprehensive atlas of the physical interactome of *Saccharomyces cerevisiae*. Mol Cell Proteomics 2007;6:439–50.

Cross FR. Two redundant oscillatory mechanisms in the yeast cell cycle. Dev Cell 2003;4:741–52.

Cross FR, Jacobson MD. Conservation and function of a potential substrate-binding domain in the yeast Clb5 B-type cyclin. Mol Cell Biol 2000;20:4782–90.

Cross FR, Yuste-Rojas M, Gray S, Jacobson MD. Specialization and targeting of B-type cyclins. Mol Cell 1999;4:11–9.

Cross FR, Archambault V, Miller M, Klovstad M. Testing a mathematical model of the yeast cell cycle. Mol Biol Cell 2002;13:52–70.

Cross FR, Schroeder L, Bean JM. Phosphorylation of the Sic1 inhibitor of B-type cyclins in *Saccharomyces cerevisiae* is not essential but contributes to cell cycle robustness. Genetics 2007;176:1541–55.

Deshaies RJ. Phosphorylation and proteolysis: partners in the regulation of cell division in budding yeast. Curr Opin Genet Dev 1997;7:7-16.

Deshaies RJ, Ferrell Jr JE. Multisite phosphorylation and the countdown to S phase. Cell 2001;107:819–22.

Escote X, Zapater M, Clotet J, Posas F. Hog1 mediates cell-cycle arrest in G1 phase by the dual targeting of Sic1. Nat Cell Biol 2004;6:997-1002.

Feldman RM, Correll CC, Kaplan KB, Deshaies RJ. A complex of Cdc4p, Skp1p, and Cdc53p/cullin catalyzes ubiquitination of the phosphorylated CDK inhibitor Sic1p. Cell 1997;91:221–30.

Fitch I, Dahmann C, Surana U, Amon A, Nasmyth K, Goetsch L, et al. Characterization of four B-type cyclin genes of the budding yeast *Saccharomyces cerevisiae*. Mol Biol Cell 1992;3:805–18.

Futcher B. Cyclins and the wiring of the yeast cell cycle. Yeast 1996;12:1635–46.

Gavin AC, Aloy P, Grandi P, Krause R, Boesche M, Marzioch M, et al. Proteome survey reveals modularity of the yeast cell machinery. Nature 2006;440:631–6.

Ghaemmaghami S, Huh WK, Bower K, Howson RW, Belle A, Dephoure N, et al. Global analysis of protein expression in yeast. Nature 2003;425:737–41.

Gunawardena J. Multisite protein phosphorylation makes a good threshold but can be a poor switch. Proc Natl Acad Sci U S A 2005;102:14617–22.

Harper JW. A phosphorylation-driven ubiquitination switch for cell-cycle control. Trends Cell Biol 2002;12:104–7.

Hochstrasser M. Ubiquitin, proteasomes, and the regulation of intracellular protein degradation. Curr Opin Cell Biol 1995;7:215–23.

Hollenhorst PC, Bose ME, Mielke MR, Muller U, Fox CA. Forkhead genes in transcriptional silencing, cell morphology and the cell cycle. Overlapping and distinct functions for FKH1 and FKH2 in *Saccharomyces cerevisiae*. Genetics 2000;154:1533–48.

Honey S, Schneider BL, Schieltz DM, Yates JR, Futcher B. A novel multiple affinity purification tag and its use in identification of proteins associated with a cyclin-CDK complex. Nucleic Acids Res 2001;29:E24.

Ingalls BP, Sauro HM. Sensitivity analysis of stoichiometric networks: an extension of metabolic control analysis to non-steady state trajectories. J Theor Biol 2003;222:23–36.

Irniger S, Piatti S, Michaelis C, Nasmyth K. Genes involved in sister chromatid separation are needed for B-type cyclin proteolysis in budding yeast. Cell 1995;81:269–78.

Jackson LP, Reed SI, Haase SB. Distinct mechanisms control the stability of the related S-phase cyclins Clb5 and Clb6. Mol Cell Biol 2006;26:2456–66.

King RW, Glotzer M, Kirschner MW. Mutagenic analysis of the destruction signal of mitotic cyclins and structural characterization of ubiquitinated intermediates. Mol Biol Cell 1996;7:1343–57.

Klein P, Pawson T, Tyers M. Mathematical modeling suggests cooperative interactions between a disordered polyvalent ligand and a single receptor site. Curr Biol 2003;13:1669–78.

Knapp D, Bhoite L, Stillman DJ, Nasmyth K. The transcription factor Swi5 regulates expression of the cyclin kinase inhibitor p40SIC1. Mol Cell Biol 1996;16:5701–7.

Koch C, Nasmyth K. Cell cycle regulated transcription in yeast. Curr Opin Cell Biol 1994;6:451–9.

Krogan NJ, Cagney G, Yu H, Zhong G, Guo X, Ignatchenko A, et al. Global landscape of protein complexes in the yeast *Saccharomyces cerevisiae*. Nature 2006;440:637–43.

Kumar R, Reynolds DM, Shevchenko A, Goldstone SD, Dalton S. Forkhead transcription factors, Fkh1p and Fkh2p, collaborate with Mcm1p to control transcription required for M-phase. Curr Biol 2000;10:896–906.

Lengronne A, Schwob E. The yeast CDK inhibitor Sic1 prevents genomic instability by promoting replication origin licensing in late G1. Mol Cell 2002;9:1067–78.

Lew DJ, Reed SI. A cell cycle checkpoint monitors cell morphogenesis in budding yeast. J Cell Biol 1995;129:739–49.

Longtine MS, McKenzie III A, Demarini DJ, Shah NG, Wach A, Brachat A, et al. Additional modules for versatile and economical PCR-based gene deletion and modification in *Saccharomyces cerevisiae*. Yeast 1998;14:953–61.

Lopez-Aviles S, Kapuy O, Novak B, Uhlmann F. Irreversibility of mitotic exit is the consequence of systems-level feedback. Nature 2009;459:592–5.

Mangus DA, Amrani N, Jacobson A. Pbp1p, a factor interacting with *Saccharomyces cerevisiae* poly(A)-binding protein, regulates polyadenylation. Mol Cell Biol 1998;18:7383–96.

Miller ME, Cross FR. Cyclin specificity: how many wheels do you need on a unicycle? J Cell Sci 2001;114:1811–20.

Nash P, Tang X, Orlicky S, Chen Q, Gertler FB, Mendenhall MD, et al. Multisite phosphorylation of a CDK inhibitor sets a threshold for the onset of DNA replication. Nature 2001;414:514–21.

Nasmyth K. At the heart of the budding yeast cell cycle. Trends Genet 1996;12:405–12.

Nishizawa M, Kawasumi M, Fujino M, Toh-e A. Phosphorylation of Sic1, a cyclin-dependent kinase (Cdk) inhibitor, by Cdk including Pho85 kinase is required for its prompt degradation. Mol Biol Cell 1998;9:2393–405.

Nugroho TT, Mendenhall MD. An inhibitor of yeast cyclin-dependent protein kinase plays an important role in ensuring the genomic integrity of daughter cells. Mol Cell Biol 1994;14:3320–8.

Pathak R, Blank HM, Guo J, Ellis S, Polymenis M. The Dcr2p phosphatase destabilizes Sic1p in *Saccharomyces cerevisiae*. Biochem Biophys Res Commun 2007;361:700–4.

Peters JM. The anaphase promoting complex/cyclosome: a machine designed to destroy. Nat Rev Mol Cell Biol 2006;7:644–56.

Pic-Taylor A, Darieva Z, Morgan BA, Sharrocks AD. Regulation of cell cycle-specific gene expression through cyclin-dependent kinase-mediated phosphorylation of the forkhead transcription factor Fkh2p. Mol Cell Biol 2004;24:10036–46.

Ralser M, Albrecht M, Nonhoff U, Lengauer T, Lehrach H, Krobitsch S. An integrative approach to gain insights into the cellular function of human ataxin-2. J Mol Biol 2005a;346:203–14.

Ralser M, Nonhoff U, Albrecht M, Lengauer T, Wanker EE, Lehrach H, et al. Ataxin-2 and huntingtin interact with endophilin-A complexes to function in plastin-associated pathways. Hum Mol Genet 2005b;14:2893–909.

Reynolds D, Shi BJ, McLean C, Katsis F, Kemp B, Dalton S. Recruitment of Thr 319-phosphorylated Ndd1p to the FHA domain of Fkh2p requires Clb kinase activity: a mechanism for CLB cluster gene activation. Genes Dev 2003;17:1789–802.

Richardson H, Lew DJ, Henze M, Sugimoto K, Reed SI. Cyclin-B homologs in *Saccharomyces cerevisiae* function in S phase and in G2. Genes Dev 1992;6:2021–34.

Schwob E, Nasmyth K. CLB5 and CLB6, a new pair of B cyclins involved in DNA replication in *Saccharomyces cerevisiae*. Genes Dev 1993;7:1160–75.

Schwob E, Bohm T, Mendenhall MD, Nasmyth K. The B-type cyclin kinase inhibitor p40SIC1 controls the G1 to S transition in *S. cerevisiae*. Cell 1994;79:233–44.

Sedgwick C, Rawluk M, Decesare J, Raithatha SA, Wohlschlegel J, Semchuk P, et al. *Saccharomyces cerevisiae* Ime2 phosphorylates Sic1 at multiple PXS/T sites but is insufficient to trigger Sic1 degradation. Biochem J 2006;399:151–60.

Seufert W, Futcher B, Jentsch S. Role of a ubiquitin-conjugating enzyme in degradation of S- and M-phase cyclins. Nature 1995;373:78–81.

Sherman F. Getting started with yeast. Methods Enzymol 2002;350:3-41.

Shirayama M, Toth A, Galova M, Nasmyth K. APC(Cdc20) promotes exit from mitosis by destroying the anaphase inhibitor Pds1 and cyclin Clb5. Nature 1999;402:203–7.

Simon I, Barnett J, Hannett N, Harbison CT, Rinaldi NJ, Volkert TL, et al. Serial regulation of transcriptional regulators in the yeast cell cycle. Cell 2001;106:697–708.

Skowyra D, Craig KL, Tyers M, Elledge SJ, Harper JW. F-box proteins are receptors that recruit phosphorylated substrates to the SCF ubiquitin-ligase complex. Cell 1997;91:209–19.

Spellman PT, Sherlock G, Zhang MQ, Iyer VR, Anders K, Eisen MB, et al. Comprehensive identification of cell cycle-regulated genes of the yeast *Saccharomyces cerevisiae* by microarray hybridization. Mol Biol Cell 1998;9:3273–97.

Thornton BR, Toczyski DP. Securin and B-cyclin/CDK are the only essential targets of the APC. Nat Cell Biol 2003;5:1090–4.
Tiana G, Krishna S, Pigolotti S, Jensen MH, Sneppen K. Oscillations and temporal signalling in cells. Phys Biol 2007;4:R1-17.
Toyn JH, Johnson AL, Donovan JD, Toone WM, Johnston LH. The Swi5 transcription factor of *Saccharomyces cerevisiae* has a role in exit from mitosis through induction of the cdk-inhibitor Sic1 in telophase. Genetics 1997;145:85–96.
Tyers M, Jorgensen P. Proteolysis and the cell cycle: with this RING I do thee destroy. Curr Opin Genet Dev 2000;10:54–64.
Ubersax JA, Woodbury EL, Quang PN, Paraz M, Blethrow JD, Shah K, et al. Targets of the cyclin-dependent kinase Cdk1. Nature 2003;425:859–64.
Verma R, Feldman RM, Deshaies RJ. SIC1 is ubiquitinated in vitro by a pathway that requires CDC4, CDC34, and cyclin/CDK activities. Mol Biol Cell 1997a;8:1427–37.
Verma R, Annan RS, Huddleston MJ, Carr SA, Reynard G, Deshaies RJ. Phosphorylation of Sic1p by G1 Cdk required for its degradation and entry into S phase. Science 1997b;278:455–60.
Visintin R, Craig K, Hwang ES, Prinz S, Tyers M, Amon A. The phosphatase Cdc14 triggers mitotic exit by reversal of Cdk-dependent phosphorylation. Mol Cell 1998;2:709–18.
Wasch R, Cross FR. APC-dependent proteolysis of the mitotic cyclin Clb2 is essential for mitotic exit. Nature 2002;418:556–62.
Yeong FM, Lim HH, Wang Y, Surana U. Early expressed Clb proteins allow accumulation of mitotic cyclin by inactivating proteolytic machinery during S phase. Mol Cell Biol 2001;21:5071–81.